Chapter

An Overview of the Mafic and Felsic Monogenetic Neogene to Quaternary Volcanism in the Central Andes, Northern Chile (18-28°Lat.S)

Gabriel Ureta, Károly Németh, Felipe Aguilera, Matias Vilches, Mauricio Aguilera, Ivana Torres, José Pablo Sepúlveda, Alexander Scheinost and Rodrigo González

Abstract

Monogenetic volcanism produces small eruptive volumes with short eruption history, different chemical compositions, and relatively simple conduit. The Central Volcanic Zone of the Andes is internationally known as a natural laboratory to study volcanism, where mafic and felsic products are present. In this contribution, the spectrum of architectures, range of eruptive styles, lithological features, and different magmatic processes of the mafic and felsic monogenetic Neogene to Quaternary volcanoes from the Central Volcanic Zone of the Andes in northern Chile (18°S-28°S) are described. The major volcanic activity occurred during the Pleistocene, where the most abundant activity corresponds to effusive and Strombolian eruptions. This volcanism is characterized by external (e.g., magma reservoirs or groundwater availability) and internal (e.g., magma ascent rate or interaction en-route to the surface) conditions, which determine the changes in eruptive style, lithofacies, and magmatic processes involved in the formation of monogenetic volcanoes.

Keywords: monogenetic volcanoes, small-volume volcanoes, magmatic and hydromagmatic eruptions, Central Volcanic Zone, Altiplano-Puna

1. Introduction

Monogenetic volcanoes are the most common type of subaerial volcanoes on the Earth [1] that occur in any tectonic setting as intraplate, extensional, and subduction [2]. They can be distributed as isolated centers, monogenetic volcanic fields [3], or associated with large volcanic systems as polygenetic volcanoes or calderas [4], displaying a plumbing system relatively simple of a dispersed nature [5]. Monogenetic volcanoes are associated with small eruptions fed from one or multiple magma batches, with volumes typically ≤1 km^3 of basic to silicic composition and form over

a short period from hours to decades. Monogenetic centers can build several volcanic landforms in response to their relationship with different environmental settings [6]. They can be produced by different eruptive styles (e.g., Hawaiian, Strombolian, violent Strombolian, phreatomagmatic, Surtseyan, and effusive activity) that are determined by internal- and external- factors [7], and evidencing several magmatic processes (e.g., fractionation, mixing, contamination) [5]. Therefore, each monogenetic volcanic system is different depending on many factors (mentioned above). For this reason, current efforts around the world focus on understanding monogenetic volcanism in different scenarios, in order to provide a better understanding of this variability and to provide tools to estimate possible scenarios of future eruption [8].

The Central Volcanic Zone (CVZ) of the Andes and particularly northern Chile (18–28°S) (**Figure 1**), is an excellent natural laboratory to study monogenetic systems of changing magma compositions in time and space related to the evolution of an active continental margin, and a ~ 70 km thick orogenic crust [12]. Despite this,

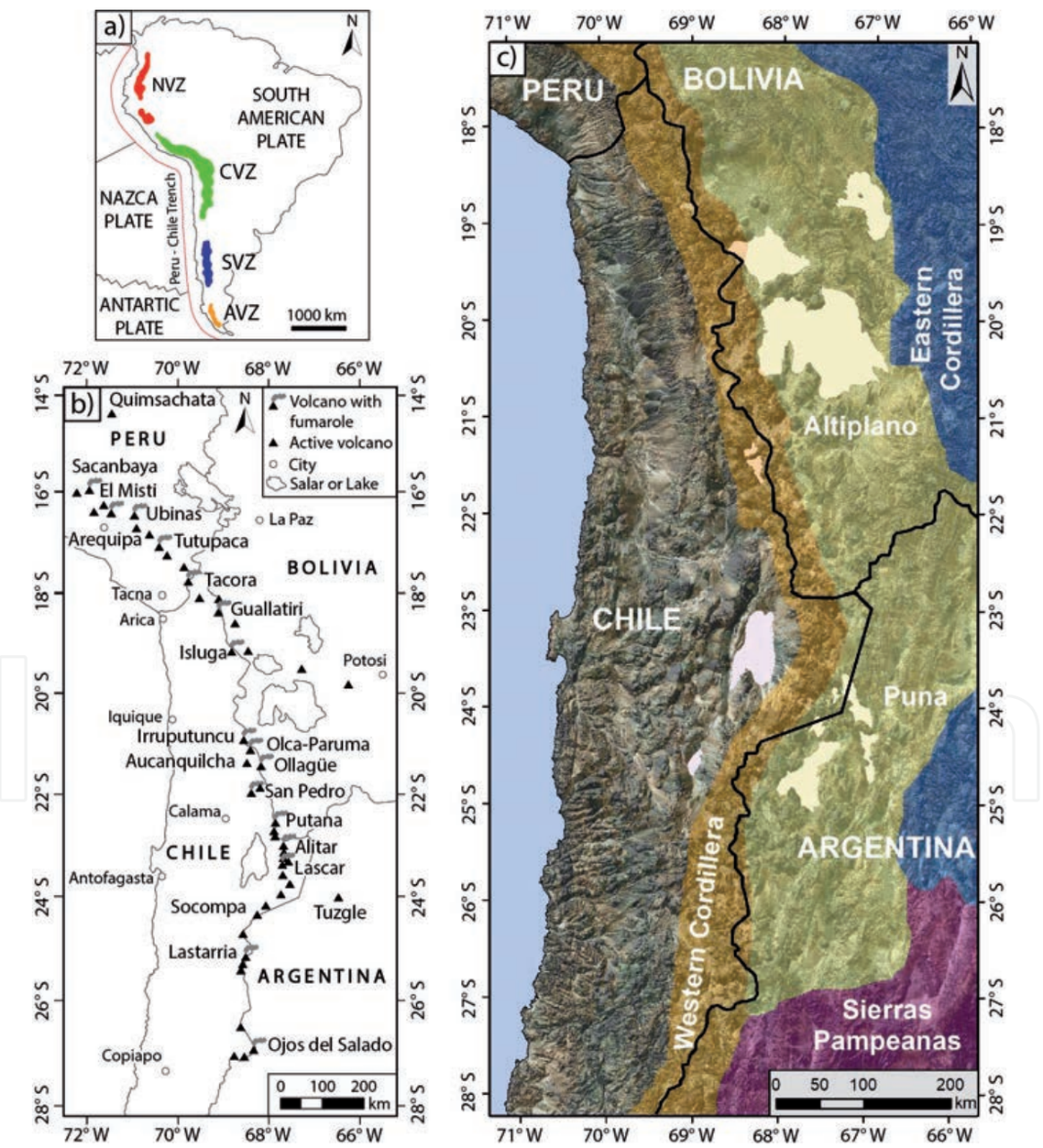

Figure 1.
a) Map showing the location of the Northern, Central, Southern, and Austral Volcanic Zones (NVZ, CVZ, SVZ, and AVZ, respectively) of the Andes defined by Thorpe and Francis [9] (modified from [10]). b) Location map of the CVZ (modified from [10]) showing the central active polygenetic volcanoes [11]. c) Map of northern Chile showing the major morpho-tectonic units of the Central Andes (modified from [12]).

prominent active polygenetic volcanoes in Chile such as Parinacota [13], Guallatiri [14], Aucanquilcha [15], Ollagüe [16], Lascar [17], Socompa [18], Lastarria [19], and Ojos del Salado [20] have received priority of research over monogenetic volcanoes (**Figure 1**). Monogenetic volcanism studies in northern Chile have rarely been mentioned, such as Chao dome [21], Tilocálar volcanoes [22], Juan de la Vega maar [23], Corral de Coquena maar [24], SC2 scoria cone [25], or Tinto dome [26]. Monogenetic volcanoes usually have been studied indirectly through i) regional geologic mapping from the Chilean Geological Service (Sernageomin); ii) only previously reported as disaggregated or preliminary data (conference papers and undergraduate thesis); iii) or by researches of a large magmatic system (such as polygenic volcanoes or calderas) mainly associated to petrological knowledge, leaving aside the mechanisms that control eruptive styles (volcanological sense) [27, 28]. Nevertheless, recently, several monogenetic volcanoes have been studied such as Cerro Chascón dome [29], Cerro Overo maar [30], La Poruña scoria cone [31], Chanka, Chac-Inca, and Pabellón domes [32], El País lava flow field [33], Tilocálar monogenetic field [34], Cerro Tujle maar [35], and many others preliminary data reports, which have increased our understanding of the monogenetic volcanism in this part of the Central Andes and provided tools to estimate possible scenarios of future eruptions that could affect the communities of the Altiplano.

In this contribution, an overview of the monogenetic volcanism that overlaps spatially and temporally the spectrum of architectures, range of eruptive styles, lithological features, and different magmatic processes of mafic and felsic monogenetic volcanoes of northern Chile (18°S-28°S) is reported. Previous studies, such as research publications and preliminary data reports, were used to assemble the volcanological, petrological, and geochronological information in the framework of this overview. A total of 907 Miocene-Quaternary monogenetic volcanoes (individual and parasite) have been identified, carefully evaluating their distribution in time and space. New stratigraphic and sedimentology data of all monogenetic volcanic center types are presented, which added to compositional and geochronological data, are used to illustrate a plumbing system model. In addition, a general eruptive model for monogenetic volcanoes in northern Chile is proposed, where external (e.g., magma reservoirs or groundwater available) and internal (e.g., magma ascent rate or interaction en-route to the surface) conditions determine the changes in eruptive style, lithofacies, and magmatic processes involved in the formation of monogenetic volcanoes. The methods used and databases generated in this contribution are available in the supplementary material.

2. Geological background

The CVZ is located between 14°S (Quimsachata, Peru) and 28°S (Ojos del Salado, Chile) of the Andean Cordillera, including southern Peru, northern Chile, southwestern Bolivia, and northwestern Argentina (**Figure 1a** and **b**). This volcanic zone is a highly elevated region, reaching a width of 350–400 km at much of it over 4000 m a.s.l., constituting the Western Cordillera and Altiplano-Puna physiographic provinces (**Figure 1c**). It is the second-highest altitude plateau in the world in size (after Tibetan Plateau of Central Asia) [36] built on a thickened continental crust that attains a maximum thickness of ~70 km [37]. The crustal thickening and high elevation of the CVZ are related to the crustal shortening [38], sub-crustal magmatism [39], delamination of eclogitic lower crust and lithosphere [40], and climatically controlled low erosion rates with limited sedimentation on the subduction trench [41]. In addition, this crustal thickness is the reason for the magma composition features that characterize the rocks that make up the CVZ as residual garnet during differentiation, crustal contamination,

melting-assimilation-storage-homogenization (MASH), and assimilation by depletion of heavy rare earth elements (HREE) in volcanic rocks [28].

The magmatic activity of the CVZ has been continuous from the Upper Oligocene to the present day [42]. The basement is mainly comprised by i) Paleozoic, Mesozoic, and Miocene-Oligocene continental volcanic and sedimentary rocks; ii) Paleozoic and Mesozoic marine sedimentary rocks; iii) Precambrian and Paleozoic metamorphic rocks; and iv) Paleozoic, Mesozoic, and Paleocene intrusive rocks ([43] and references therein).

The Central Andes is known as the home of "andesitic" magmatism [36]; nevertheless, lava and pyroclastic rocks of dacitic, rhyolitic, and occasionally basaltic andesite and basaltic composition volcanic rocks also occur in the CVZ, building calderas, extensive ignimbrite sequences, stratovolcanoes and monogenetic volcanoes [44].

3. Volcano-tectonic implications: the relationship between vent locations and the structural elements

In this study, 907 monogenetic volcanic centers were identified in northern Chile (**Figure 2**). Among which, 306 centers correspond to parasitic monogenetic volcanoes associated with polygenetic volcanoes (**Figure 2a**), which are at the flank of stratovolcanoes linked to crustal/edifice magma storage [45], and 601 centers correspond to individual monogenetic volcanoes (**Figure 2a**). The monogenetic centers

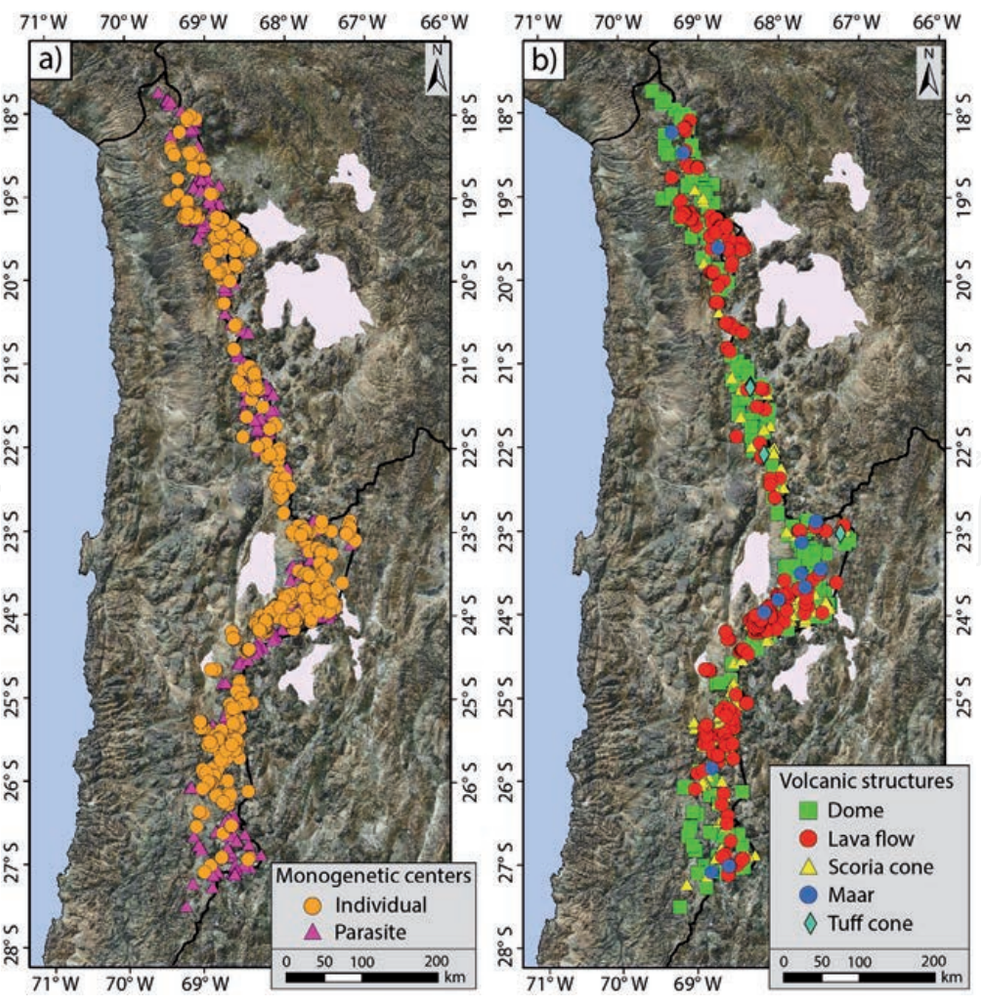

Figure 2.
Distribution of monogenetic volcanoes across northern Chile based on a) their relationship with polygenetic volcanoes and b) their volcanic landform.

show a variety of volcanic structures such as domes (35.1%), lava flows (33.4%), scoria cones (29.6%), maars (1.5%), and tuff cones (0.4%) (**Figure 2b**). These centers can be found as isolated centers (e.g., Cerro Punta Negra), clusters (e.g., Purico-Chaskón complex), or forming small volcanic fields (e.g., Negros de Aras).

Using the location of the total number of the monogenetic volcanoes (i.e. 905), the average nearest neighbor analysis can be used to differentiate the distribution of each kind of monogenetic landforms (e.g., [3, 46]). The average nearest neighbor analysis shows R-statistic values of 0.71 for all monogenetic volcanoes of northern Chile, 0.74 for domes, 0.69 for scoria cones, and 0.62 for lava flows (**Table 1**). These value ranges are identified as a clustered distribution of volcanic centers [46]. For maars and tuff cones, the average nearest neighbor analysis was not obtained due to the small number of centers identified (18 monogenetic centers that are 1.9% of the total) to generate a statistically significant result.

On the other hand, using the total number of monogenetic volcanoes (i.e. 907) and the area in which the monogenetic volcanoes are distributed in northern Chile (46,610 km^2), the area that envelopes all the monogenetic volcanic centers identified is of 1.95 x 10^{-2} centers/km^2. The temporal distribution is characterized by a decrease in eruptive centers from Miocene (268 monogenetic centers) to Pliocene (258 monogenetic centers), and a later increase in the Pleistocene (363 monogenetic centers) (**Figure 3**). Domes and scoria cones abundance show the same trend mentioned before, whereas lava flows, maars, and tuff cones display a trend to increase from Miocene to Pleistocene (**Figure 3**). The activity during the Holocene (18 monogenetic centers) is mainly dominated by dome eruptions (**Figure 3**).

The temporal evolution of the monogenetic volcanoes from older to younger shows a migration from south to north with a concentration in the central part of northern Chile (cluster 3: Antofagasta Central). Based on the kernel density map, the monogenetic volcanoes of northern Chile may be mainly grouped into five regional clusters (**Figure 4a**). These distributions of volcanic centers display a high density of features and a preferred elongation trending. Monogenetic centers are alienated NW-SE preferentially for clusters 1 and 2, N-S, NW-SE, and NE–SW for cluster 3, NE–SW for cluster 4, and WNW-ESE and NW-SE for cluster 5 (**Figure 4a**). The volcanic structures distribution across the northern Chile map (**Figure 4b**) exhibits that scoria cones and domes are mainly associated with NNW–SSE, NW-SE, and WSW-ENE tectonic structures and lineaments, in decreasing order of frequency. Lava flows are mainly aligned N-S and NW-SE, while maars and tuff cones occur mainly along N-S, NW-SE, and WSW-ENE trending tectonic structures and lineaments, in decreasing order of frequency. The distribution of magma paths suggests that for Miocene, the main direction of the shortening of structures at the upper crust should have been about E-W, WNW-ESE, and NNW–SSE [47]. This is consistent with the development of N-S and NNE–SSW reverse faults and folds reported for cluster 2 (Antofagasta Norte; **Figure 4a**), cluster 3 (Antofagasta Central; **Figure 4a**) and cluster 4 (Antofagasta Sur; **Figure 4a**), and WSW-ENE structures for cluster 5

Feature	Ro (km)	Re (km)	R-statistic	ZR	Pattern
All monogenetic structures	2.56	3.61	0.71	−16.63	Clustered
Domes	4.51	6.05	0.74	−8.71	Clustered
Lava flows	3.85	6.2	0.62	−12.62	Clustered
Scoria cones	4.57	6.45	0.69	−9.48	Clustered

Ro: Observed Mean Distance; Re: Expected Mean Distance; R-statistic: Nearest Neighbor Ratio; ZR: Z-score.

Table 1.
Results for the average nearest neighbor in northern Chile.

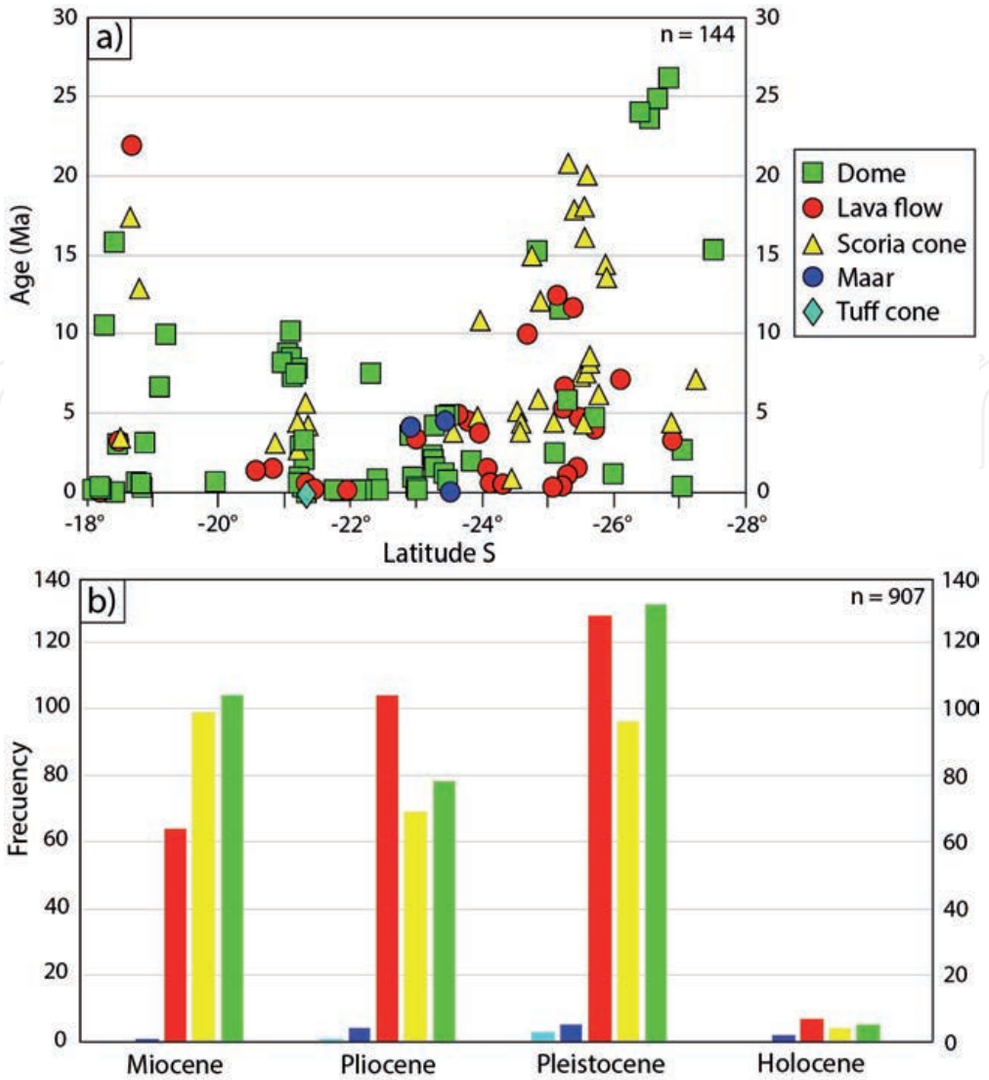

Figure 3.
a) Temporal distribution of monogenetic volcanic landforms across northern Chile. b) Histogram of the temporal distribution of monogenetic volcanic landforms during Miocene, Pliocene, Pleistocene, and Holocene.

(Atacama; **Figure 4a**) in previous studies [48]. During the Pliocene to Holocene, the main direction of shortening inferred to have been E-W, NE–SW, WNW-ESE, and NNW–SSE direction of contraction, in decreasing order of frequency. This is consistent with the N-S and NW-striking normal faults, NE-striking reverse faulting, NW-SE, and WSW-ENE strike-slip faults reported in previous studies [20, 48].

The spatial–temporal correlation of monogenetic centers, combined with the tectonic structures within northern Chile, allows the identification of three different structural styles of monogenetic volcanoes (Figure A.1), as has been suggested by Le Corvec et al. [2] for monogenetic volcanism and by Tibaldi et al. [49] for the CVZ. The first case (Figure A.1a) corresponds to a compressional environment mainly characterized by N-S and NNE–SSW reverse faults and folds over the monogenetic feeding conduits. Nevertheless, in this case, the magmatic plumbing system has been associated with the development of normal or strike-slip faults allowing the ascent of magmas to the surface such as the Tilocálar complex [22] at the south of the Salar de Atacama basin into the cluster 3 (Antofagasta Central; **Figure 4**). The second scenario (Figure A.1b) is mainly characterized by N-S and NW-SE, striking normal faults into an extensional environment. This case has been reported to scoria cones, lava flows, and mainly domes into the Ollagüe region and San Pedro-Linzor volcanic chain area [16, 50], which correspond to cluster 2 (Antofagasta Norte; **Figure 4**). The last scenario (Figure A.1c) corresponds to a strike-slip environment mainly

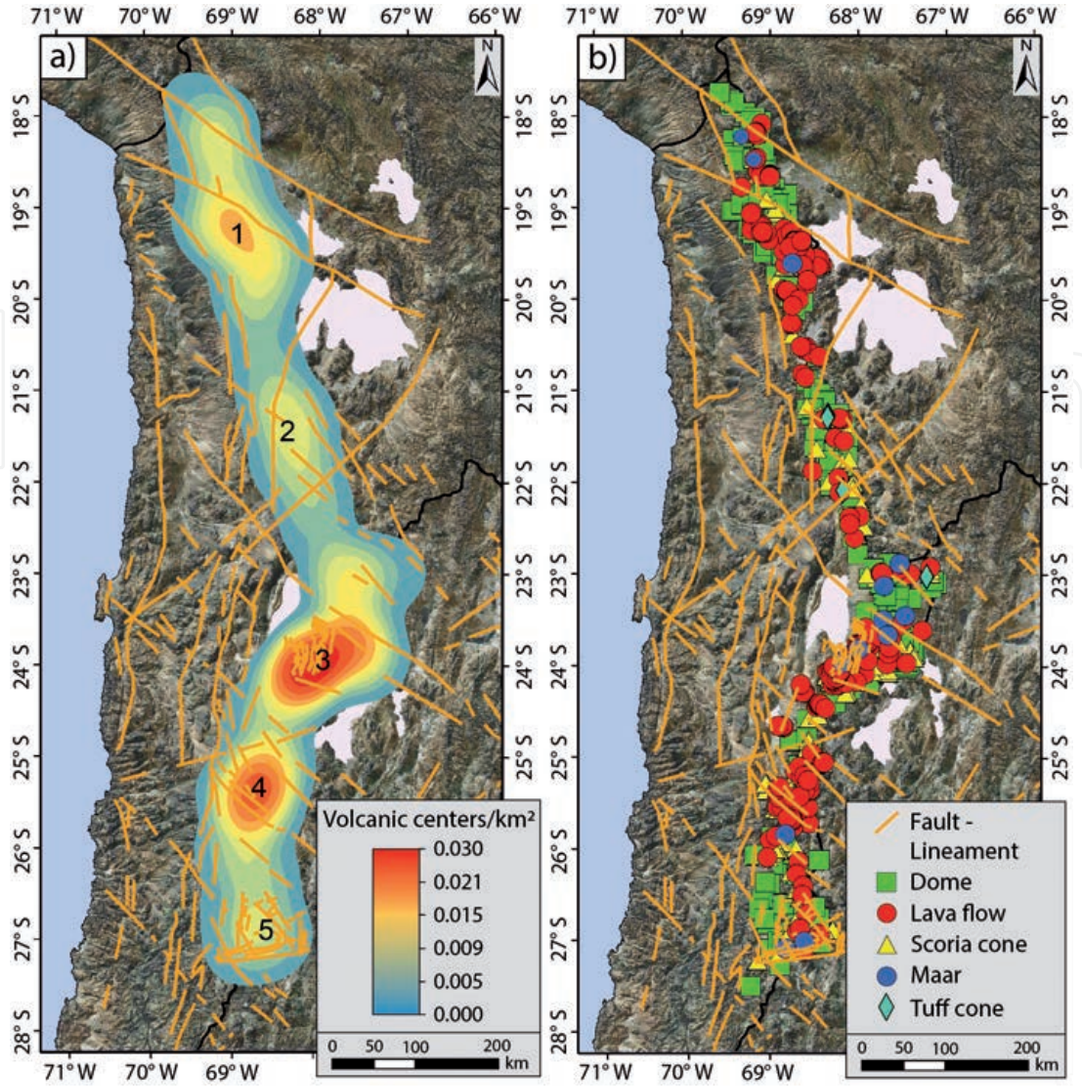

Figure 4.
a) Kernel density map for monogenetic volcanoes and the main clusters identified. The numbers represent the main regions: 1. Arica-Iquique, 2. Antofagasta Norte, 3. Antofagasta Central, 4. Antofagasta Sur, and 5. Atacama. b) Map of the major fault systems and lineaments across northern Chile.

characterized by NW-SE left lateral and WSW-ENE strike-slip faults. Monogenetic volcanism associated with this scenario has been mainly reported by Tibaldi et al. [49] for cluster 3 (Antofagasta Central; **Figure 4**), Baker et al. [20], and González-Ferrán et al. [51] for cluster 5 (Atacama; **Figure 4**). These scenarios have also been reported in others areas of monogenetic volcanism in the CVZ of the Andes such as the Uyuni region by Tibaldi et al. [50], Antofagasta de la Sierra Basin by Báez et al. [52], or in the southern Puna Plateau by Haag et al. [3]. These interpretations were developed based on the distribution and alignment of the monogenetic centers. Therefore, it is essential to consider that the tectonic structures have been formed before of the magma intrusion that originated monogenetic centers. In this context, the emplacement of these volcanic centers was favored by these tectonic structures.

4. The spectrum of architecture and lithofacies of volcanic structures: internal versus external-factor implications

In this study, 318 domes, 303 lava flows, 268 scoria cones, 14 maars, and 4 tuff cones have been identified. This identification is primarily based on the morphological aspects of the volcanic edifices, which is characterized by the dominant

eruption style and number or combination of eruption phases following Bishop [53] and Walker [54] (**Figures 1** and **2**).

Scoria cones (**Figure 5a**) are mainly characterized by circular to elliptical shape in plan-view, showing different landforms as ideal (e.g., La Poruña), gully, horseshoe, tilted, amorphous or crater row that in some cases display lava flows associated (e.g., Negros de Aras volcanic field). These lava flows (**Figure 5b**) are mainly characterized by ʻaʻā flow structures associated with early (e.g., Del Inca) or late-stage (e.g., Ajata) eruptions with channel, ogive, leeve, lobe, and breakout lobe structures.

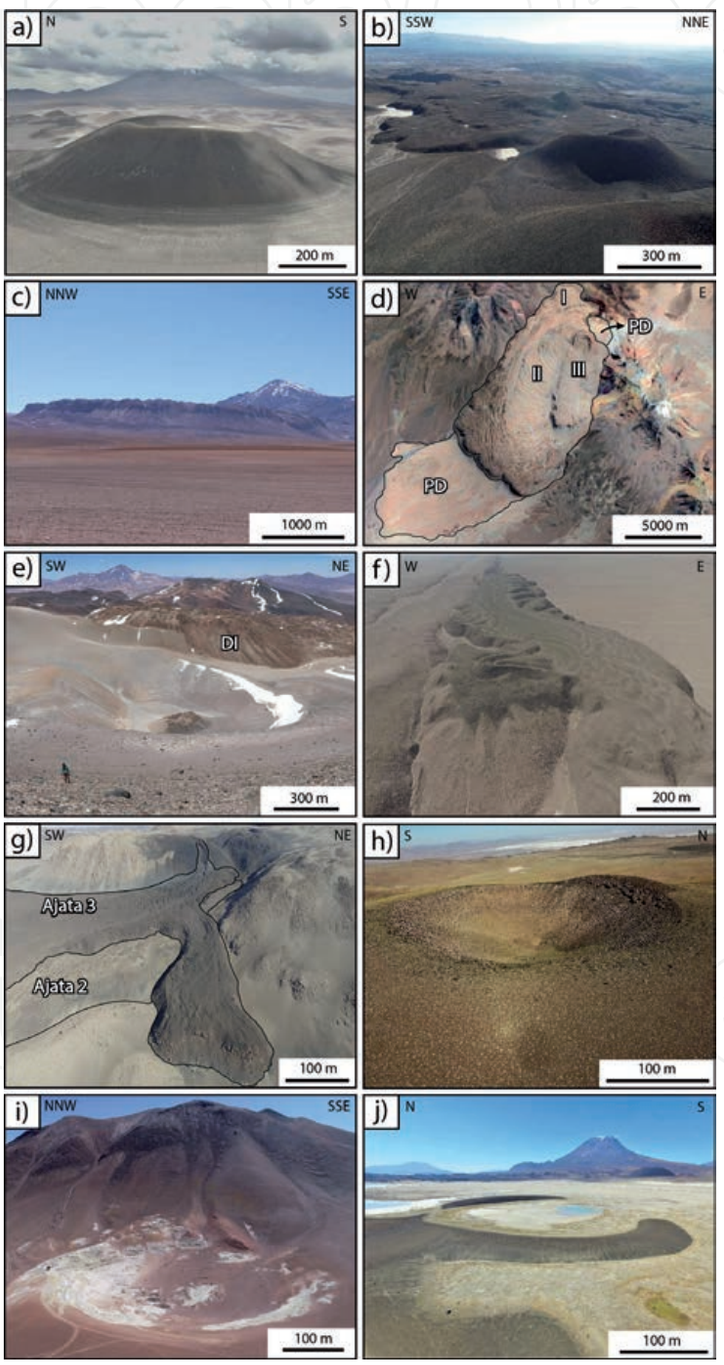

Figure 5.
Volcano types from northern Chile. a) Poruñita scoria cone (Ollagüe stratovolcano in the background). b) Scoria cone and lava flows from Negros de Aras monogenetic volcanic field. c) La Torta de Tocorpuri dome. d) Chao dome with its pyroclastic deposit (PD) and lava dome stages (I, II, and III) (Google earth™ image). e) La Espinilla maar-dome and Del Indio dome (DI). f) Tilocálar Norte lava flow. g) Ajata lava flows. h) Cerro Tujle maar. i) Alitar maar, fumaroles occur in white areas (Alitar stratovolcano in the background). j) Luna de Tierra tuff cone (Ollagüe stratovolcano in the background).

Domes (**Figure 5c**) of northern Chile are characterized by a pile up of lava in large thicknesses over their vents. They are often referred to as *tortas* (pies or pancakes) (e.g., La Torta de Tocorpuri), controlled by the slope angle of the pre-eruptive surface, viscosity, effusion rate, phenocryst contents, and in some cases, related to early pyroclastic density currents (e.g., Chao). Overall, domes (**Figure 5d**) show coulee (e.g., Chao), lobate (e.g., Chascón), platy (e.g., Pabellón-Apacheta), and axisymmetric (e.g., Chillahuita) landform structures. Few domes (**Figure 5e**) in northern Chile occur within craters (e.g., La Espinilla).

Lava flows (**Figure 5f**) are mainly characterized by a jumble of irregular and coherent block of lava (up to meters), across with smooth, planar, and angular surfaces. They can be classified as ʻaʻā (e.g., El Negrillar) and blocky (e.g., Tilocálar Norte) lavas, and may display a simple (e.g., Ajata) or compound (e.g., Tilocálar Sur) landform with several features as a channel, ogive, leeve, lobe, and breakout lobe structures (**Figure 5g**).

Maars (**Figure 5h**) show a characteristic landform characterized by a preserved crater that cut into the pre-eruptive landscape (e.g., Tujle). The crater cavities reach from 30 m to 200 m deep; they are partially sediment filled with a crater diameter from 300 m to 3 km. Sulfur deposits (e.g., Juan de la Vega maar), fumaroles (e.g., Alitar maar), and domes (e.g., La Espinilla) are present in maar volcanoes associated with events that appear late of the maar eruptions (**Figure 5e–i**).

Tuff cones (**Figure 5j**) in northern Chile display a horseshoe landform, a wider crater relative to basal diameter than the scoria cones, exhibiting a crater rim from a flat surface up to 10 m dominated by salt deposits. They are mainly associated with salt plains or *salares* (e.g. Luna de Tierra).

The monogenetic volcanic centers (mafic and felsic volcanism) are characterized by the heterogeneity of volcanic products, which can be mainly classified into eight lithofacies based on field observation, componentry and sedimentological characteristics such as:

1. *Bombs and lapilli beds* (BL): This lithofacies is mainly found both at the base and the summit of scoria cones. It is poorly sorted, reversed graded to massive and mostly clast-supported, and consists of poorly to non-agglutinated juvenile clasts (**Figure 6a** and **b**). BL lithofacies is interpreted as the result of Strombolian eruptions.

2. *Lapilli and ash beds* (LA): This lithofacies is mainly located at the base of scoria cones. It is well sorted, normal or reversed graded to massive, with parallel or cross-lamination, and mostly clast-supported with non-agglutinated juvenile clasts (**Figure 6c**). This lithofacies is interpreted as the result of hydromagmatic eruptions.

3. *Agglutinated to spatter bomb and lapilli beds* (AS): This lithofacies is mainly found at the summit of scoria cones or pyroclastic deposits. It comprises a brittle core and fluid rim to completely fluid clasts (spatter) that agglutinate moderately forming beds (up to 5 m thick) (**Figure 6d**). LA lithofacies is interpreted as the result of Hawaiian to transitional eruptions.

4. *Welded scoria to clastogenic lavas* (CL): This lithofacies is mainly located at the summit of scoria cones and pyroclastic deposits. It is formed by scoria of lapilli and bombs size fragments highly welded (coalesced), forming dense agglutinate layers (clastogenic lava) (**Figure 6e**). CL lithofacies is interpreted as the result of Hawaiian to transitional eruptions.

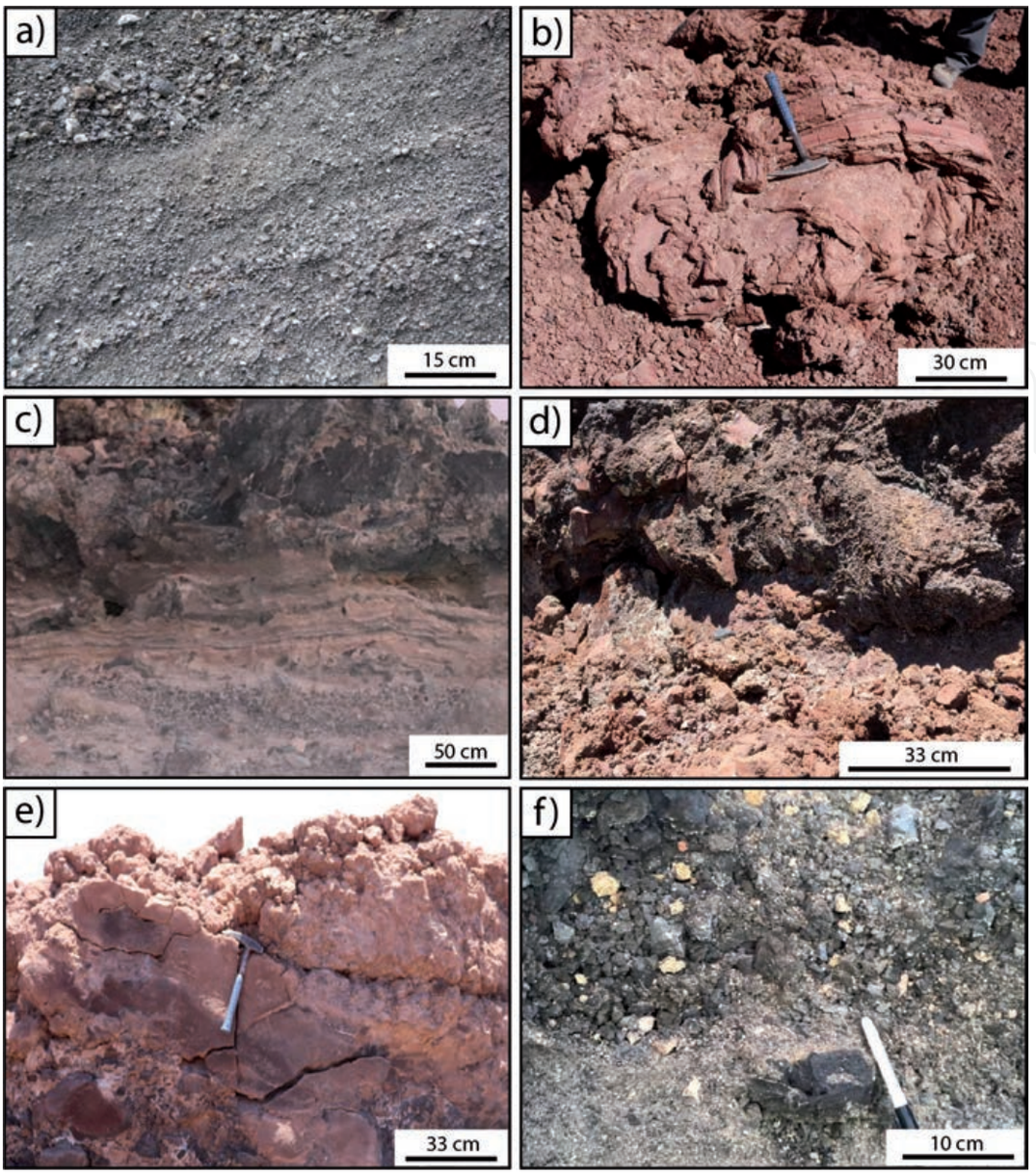

Figure 6.
Field photographs of lithofacies of the monogenetic volcanoes in northern Chile. a) Lithofacies BL from Poruñita scoria cone. b) Lithofacies BL from La Poruña scoria cone. c) Lithofacies LA from Negros de Aras scoria cones. d) Lithofacies AS from Ajata scoria cone. e) Lithofacies CL from Tilocálar Sur pyroclastic deposit. f) Lithofacies LAL from Cerro Overo maar.

5. *Lapilli and ash beds with lithic fragments* (LAL): This lithofacies is mainly found both at the base and the summit of scoria cones and pyroclastic deposits. It is moderately sorted, normal or reversed graded to massive and mostly clast-supported deposits with abundant lithic fragments (>20%) locally moderate to no agglutination/welding (**Figures 6f** and **7a**). LAL lithofacies is interpreted as the result of hydromagmatic eruptions.

6. *Peperite* (P): This lithofacies is located at the base of scoria cones and pyroclastic deposits, overlying the pre-eruptive surface. It is mainly a mingling of juvenile material and unconsolidated host sediment (**Figure 7b**). P lithofacies is interpreted as the result of magma-wet sediment/shallow water eruptions.

7. *Lava flow* (LF): This lithofacies is found at the flank and ring plain of strato-volcanoes, both at the base and at the summit of scoria cones (from *boccas*) (**Figure 7c** and **d**), at the crater of other volcanic edifices (polygenetic or

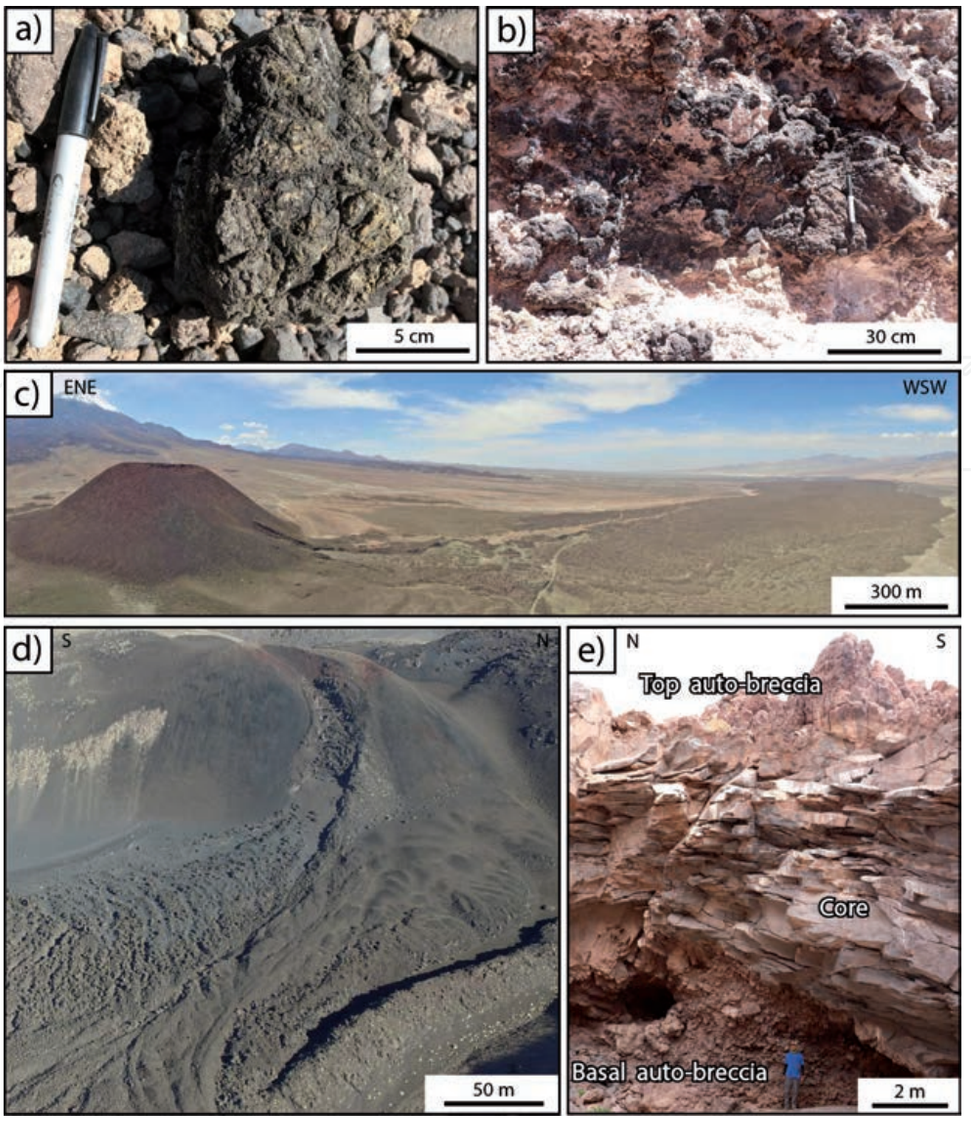

Figure 7.
Field photographs of lithofacies of the monogenetic volcanoes in northern Chile. a) Lithofacies LAL showing a juvenile fragment with cauliflower-shaped from Cerro Overo maar. b) Lithofacies P showing a mingling of juvenile material and unconsolidated host sediment from Tilocálar Sur pyroclastic deposit. c) La Poruña lava flow and scoria cone. d) Lithofacies LD showing the boccas *of the Ajata scoria cone with levee structures of the Ajata 3 lava flow. e) Lithofacies LD showing the primary three principal levels of this lithofacies (top auto-breccia, core, and basal auto-breccia) from El País lava flow field.*

monogenetic), and as an isolated vent. Lava flow lithofacies is characterized by three primary vertical levels (**Figures 7e** and **8a–e**). This lithofacies flowed, reaching length up to 11 km and piling up from low to large thicknesses (< 1 m – 400 m), and based on their morphology, it can be classified as lava flows or domes. LF lithofacies is mainly interpreted as the result of Strombolian eruptions.

8. *Raft blocks* (RB): This lithofacies corresponds to mounds or blocks of agglutinate to welded pyroclasts located on top of lava flows and associated with scoria cones (**Figure 8f** and **g**). The individual blocks are the result of the cone rafting (RB lithofacie), which initially were the product of Strombolian style eruptions.

The spectrum of architecture and lithofacies of volcanic structures involve several interactions between internal and external processes. It is affected by the continuous degassing and interactions of the magma with the environment at different levels en-route during its ascent from the source to the surface, resulting in a volcanic eruption that can be explosive or effusive [55]. In many cases,

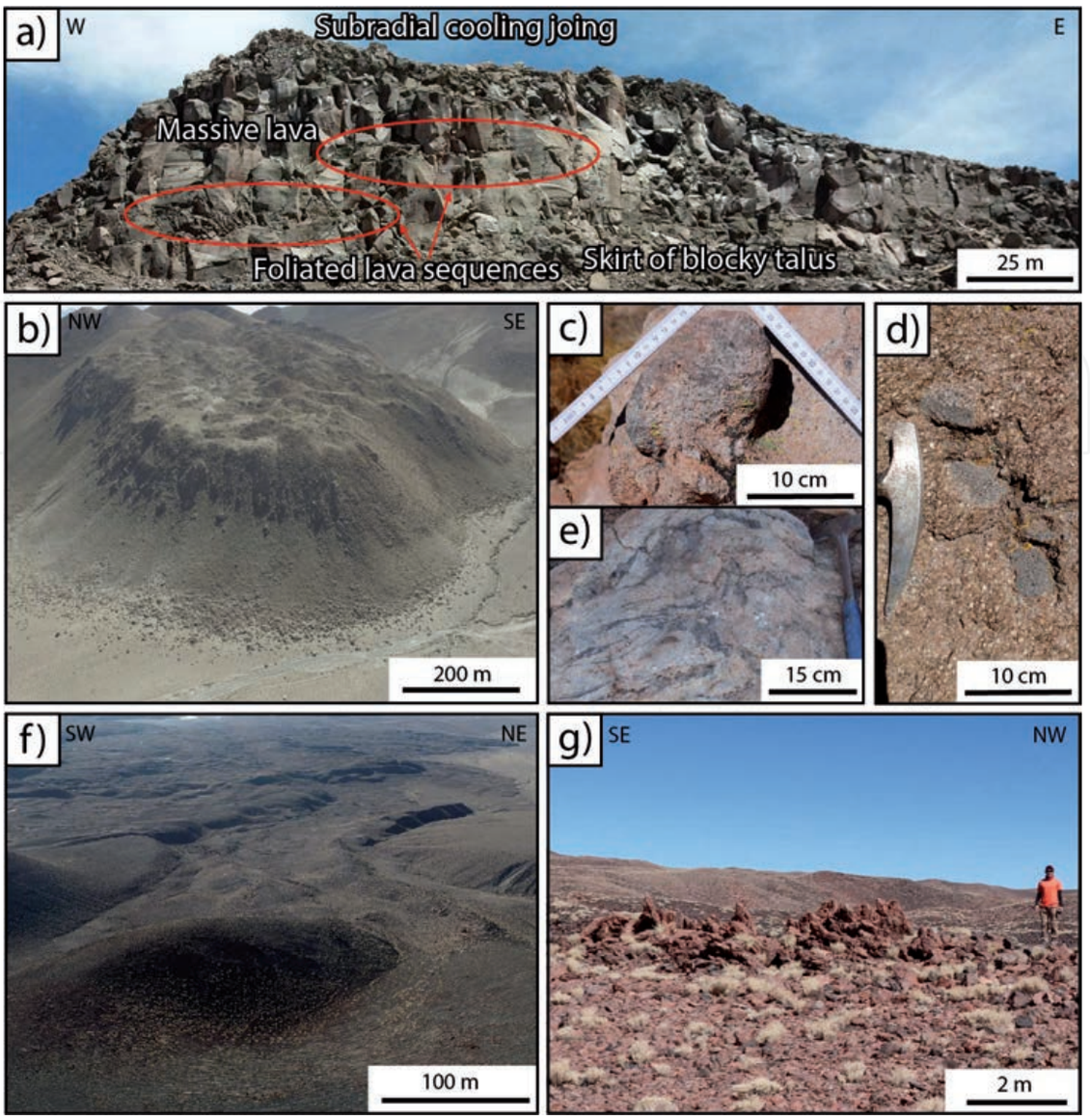

Figure 8.
Field photographs of lithofacies of the monogenetic volcanoes in northern Chile. a) South dome (Guallatiri volcano area) showing the three primary levels of this lithofacies. Red areas indicate foliated lava sequences that are described in Watts et al. [26] in ref.s therein. b) El Ingenio (also called La Celosa) felsic dome (Ollagüe volcano area) exhibiting a torta *type morphology. c-d) mafic enclaves from El Ingenio dome and south dome, respectively. e) Flow structures of El Mani dome. f) Scoria cone from Negros de Aras showing a horseshoe morphology associated with lava flow and with agglutinated material deposited on the summit crater. g) Lithofacies RB of unconsolidated and agglutinated pyroclastic material located at the distal part of the lava flow of* ***Figure 8f*** *from Negros de Aras.*

the outcrops of monogenetic volcanic centers are covered by some debris flank due to desert physical weathering and mass movements or covered by eolian deposits. Nevertheless, integrating the different lithofacies identified and the cross-sections from different edifices are possible to build the history of the eruptive style involved in the formation of the monogenetic volcanoes of northern Chile.

In general, scoria cones are composed of the lithofacies that indicate a rapid and continuous evolution from the Strombolian eruption style (lithofacies BL) to Hawaiian and Transitional styles (lithofacies AS and CL). This transition is characterized from the base to the upper levels by poorly sorted, reversed graded to massive and mostly clast-supported deposits, which consist of poorly to non-agglutinated juvenile clasts, to the summit by clastogenic lavas and welded agglutinated bomb (e.g., Ajata, La Poruña, Del Inca, Negros de Aras scoria cones). In addition, magmatic effusive stages are associated with the lithofacies LF (lava flow)

and RB (raft blocks). They are represented by lava flows at the base or the summit of the scoria cones (e.g., Ajata, La Poruña, Del Inca, Negros de Aras scoria cones), and mounts from the volcanic edifice of scoria cones at the lava flows (e.g., Negros de Aras), respectively. That means scoria cones show a range of magmatic activity from explosive to effusive styles (**Figure 9**).

Nevertheless, in some cases (e.g., Negros de Aras scoria cones), hydrovolcanic records may be identified either at the summit or at the bases of the scoria cones (**Figure 9**). This corresponds to the lithofacies LAL (lapilli and ash beds with lithic fragments) and LA (Lapilli and ash beds), which suggest magma-water interactions during the initial (e.g., Poruñita scoria cone) or later phases (e.g., Negros de Aras scoria cones), where shallow water levels are available. This characteristic is also recognized at the base in some pyroclastic deposits (e.g., Tilocálar Sur), where fluidal and jigsaw-fit textures are locally preserved (lithofacies P) (**Figure 7b**).

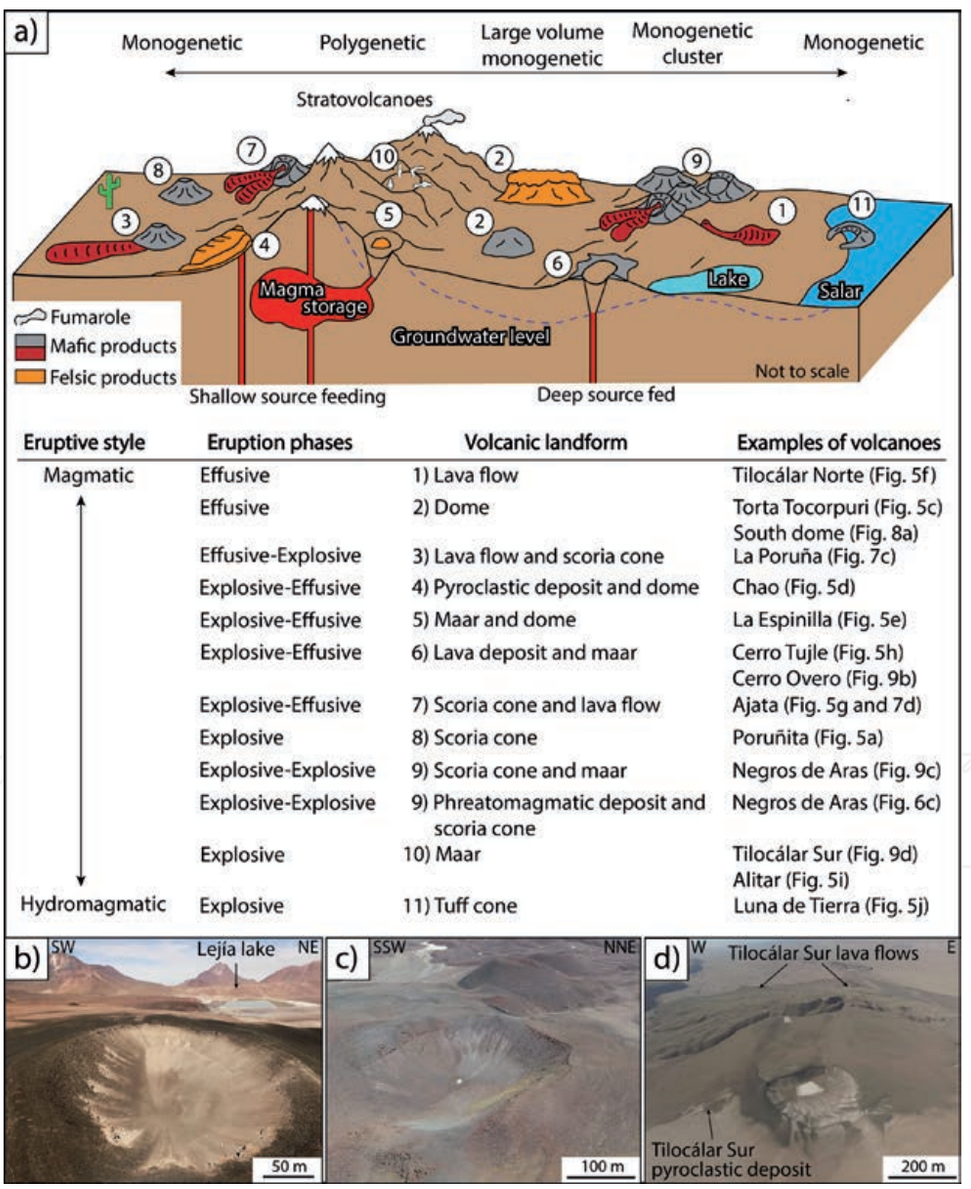

Eruptive style	Eruption phases	Volcanic landform	Examples of volcanoes
Magmatic	Effusive	1) Lava flow	Tilocálar Norte (Fig. 5f)
	Effusive	2) Dome	Torta Tocorpuri (Fig. 5c)
			South dome (Fig. 8a)
	Effusive-Explosive	3) Lava flow and scoria cone	La Poruña (Fig. 7c)
	Explosive-Effusive	4) Pyroclastic deposit and dome	Chao (Fig. 5d)
	Explosive-Effusive	5) Maar and dome	La Espinilla (Fig. 5e)
	Explosive-Effusive	6) Lava deposit and maar	Cerro Tujle (Fig. 5h)
			Cerro Overo (Fig. 9b)
	Explosive-Effusive	7) Scoria cone and lava flow	Ajata (Fig. 5g and 7d)
	Explosive	8) Scoria cone	Poruñita (Fig. 5a)
	Explosive-Explosive	9) Scoria cone and maar	Negros de Aras (Fig. 9c)
	Explosive-Explosive	9) Phreatomagmatic deposit and scoria cone	Negros de Aras (Fig. 6c)
	Explosive	10) Maar	Tilocálar Sur (Fig. 9d)
			Alitar (Fig. 5i)
Hydromagmatic	Explosive	11) Tuff cone	Luna de Tierra (Fig. 5j)

Figure 9.
a) Schematic drawing of monogenetic volcanic landforms of northern Chile, showing the conceptual link between monogenetic and polygenetic volcanoes and their relationship with their environmental setting. The numbers indicate the volcanic landforms detailed in the diagram of the theoretical link/transition between eruptive styles, eruption phases, and volcanic landforms for monogenetic volcanoes of northern Chile. Examples of Chilean volcanoes in each case. b) Cerro Overo maar. c) Scoria cone from Negros de Aras with a crater associated with a phreatomagmatic eruptive phase. d) Tilocálar Sur maar.

On the other hand, lava flows and lava domes are characterized by the lithofacies LF (lava flow), suggesting a magmatic effusive nature with different morphological features (**Figure 9**). The main differences between lava flows (e.g., El País lava flow field; **Figure 7e**) and lava domes (e.g., Tinto dome; **Figure 8a**) are the changes in the viscosity, volatile content, and magma ascent rate [55]. These features control the magma degassing during their ascent from the source to the surface, and therefore, the fragmentation processes [56]. Despite these differences, deposits that are inferred to represent explosive phases have been found at the base of the lava domes (e.g., Chao dome), which corresponds to the initial stages of pyroclastic deposits characterized by bombs and lapilli beds (lithofacies BL).

Maars (e.g., Cerro Overo) and tuff cones (e.g., Luna de Tierra) are characterized by LAL (lapilli and ash beds with lithic fragments) and LA (Lapilli and ash beds) lithofacies, which are associated with hydromagmatic eruptions, suggesting magma-water interactions. These phreatomagmatic and Surtseyan eruptions may be associated with external factors that trigger the magma-water interaction at different degrees of ratio and different depths of magma-water interaction [57]. The maars are mainly associated with areas characterized by i) folded ignimbrite basement (e.g., Tilomonte ridge for Tilocálar Sur maar, Cerro Tujle ridge for Cerro Tujle maar or Altos del Toro Blanco ridge for Cerro Overo maar), ii) groundwater aquifers (e.g., Monturaqui-Tilopozo-Negrillar aquifer for Tilocálar Sur maar), and iii) salt flats or lagoons as discharge zones (e.g., Salar de Atacama for Cerro Tujle maar or Laguna Lejía for Cerro Overo maar) (**Figure 9**). In contrast, tuff cones are located at low topographic positions filled with poorly consolidated sediments as salt flats (e.g., Salar de Carcote for Luna de Tierra) or caldera basins (e.g., La Pacana caldera for Corral de Coquena), where the resulting tephra came from phreatomagmatic eruptions through shallow surface water [58] (**Figure 9**).

Overall, the architecture spectrum and the volcanic lithofacies of the monogenetic centers of northern Chile (**Figure 9**) are similar to those reported for the northern Puna region (Argentina) by Maro and Caffe [59] and Maro et al. [60]. This suggests a wide range of eruptive styles involved in the eruption history of this small-volume volcanism, and in some cases, large volume as well. Nevertheless, in northern Chile, this range of eruptive styles is characterized by effusive (e.g., Ajata lava flows or Tinto dome) and/or explosive magmatic (e.g., Tilocálar Sur or Chao dome) activities dominated by Strombolian to Hawaiian/Transitional styles (e.g., La Poruña scoria cone), and hydromagmatic activities, as phreatomagmatic (e.g., Cerro Overo maar) or Surtseyan (e.g., Luna de Tierra tuff cone) styles, which were often simultaneous or alternating during the growth of the monogenetic volcanoes in northern Chile (**Figure 9**).

5. Magmatic processes: textural and petrological evidence

Petrographically, products from scoria cones, lava flows, maars, and tuff cones comprise mainly aphyric rocks (e.g., SC2). On the other hand, domes can be variable from aphyric (e.g., La Albondiga) to porphyritic rocks, which in some cases show mafic enclaves (e.g., Tinto dome). Overall, samples are characterized by hypocrystalline, hypidiomorphic, and hyalopilitic textures, where aphyric rocks show 40–50% vol. microphenocryst and microlite content, whereas porphyritic rocks exhibit 20–50% vol. phenocryst. The main mineral assemblage corresponds to euhedral to subhedral clinopyroxene (15% vol.; max 1.15 mm) and plagioclase (25–40% vol.; max 7 mm) with subordinated olivine (5% vol.; max 0.9 mm) and Fe–Ti oxide phases (1% vol.; max 0.2 mm). Nevertheless, in some cases, orthopyroxene (3% vol.; max 0.4 mm) and hydrous minerals, such as amphibole (**Figure 10a**),

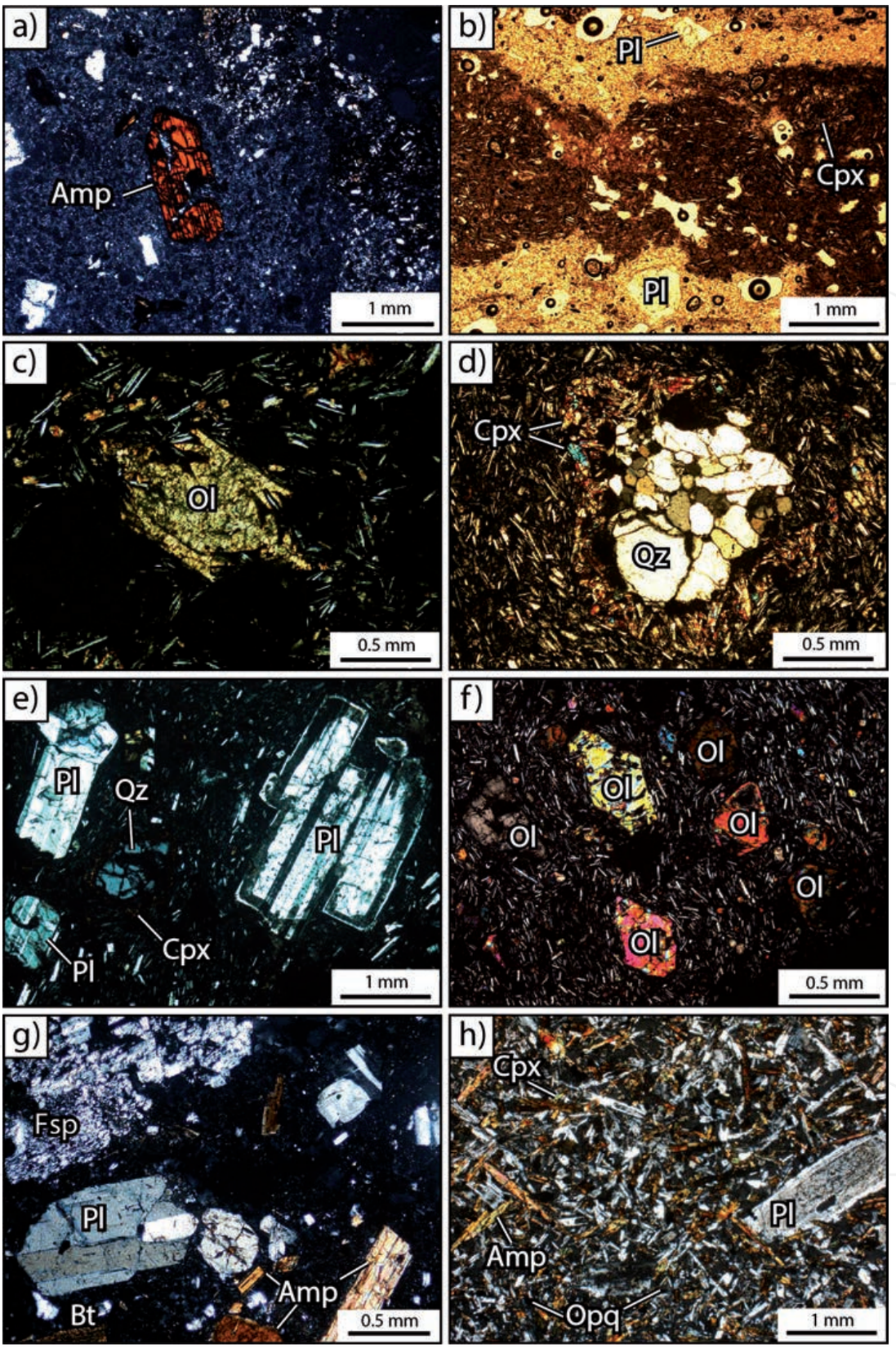

Figure 10.
Photomicrographs and micro-vesiculated photos are showing typical petrographic textures of monogenetic volcanoes products from northern Chile. Thin sections under cross-polarized- (a, c-h) and plane-parallel- (b) light. a) Amphibole breakdown/reaction rim with skeletal and sieve textures from Cerro Tujle maar. b) Mafic and felsic bands are showing mingling texture from El Maní dome. c) Olivine phenocryst showing skeletal growth from SC2 scoria cone. d) Quartz xenocryst resorbed and rimmed mainly by clinopyroxenes from Tilocálar Sur lava flow. e) Plagioclase with sieve and reabsorption textures and showing zoned rim from Luna de Tierra tuff cone. f) Fluidal texture showing olivines with absorption and skeletal growth textures from Cerro Overo maar. g) Silicic product from El Ingenio dome. h) the diktytaxitic-like texture of the groundmass of the enclave from El Ingenio dome. Mineral abbreviations are amphibole (amp), plagioclase (Pl), Clinopyroxene (Cpx), olivine (Ol), quartz (Qz), K-feldspar (Fsp), Biotite (Bt), opaque mineral (Opq).

biotite, or sideromelane (10% vol; max 5 mm) can also be found. The main textures correspond to fluidal, reabsorption, and disequilibrium textures, such as mingling (**Figure 10b**), skeletal (**Figure 10c**), and resorbed edges rimmed by a network of clinopyroxenes (**Figure 10d**), sieve texture, and zoned rims (**Figure 10e**). The groundmass (50–80% vol.) is glassy with a microlites of plagioclase > clinopyroxene > olivine > amphibole/biotite > orthopyroxene, and opaque phases, where tabular-shaped microlites display flow structures (**Figure 10f**). In general, the mafic inclusions commonly are fine-grained and microvesiculated and range from 2 to 20 cm in size (**Figure 10g**). They exhibit crystal assemblages of plagioclase, pyroxene, amphibole, biotite, olivine, and quartz. The groundmass shows mainly plagioclase > pyroxene > amphibole and rare biotite and Fe-Ti oxides, with acicular phases and diktytaxitic texture (vesicles with plagioclase around cavity; **Figure 10h**).

In general, products of monogenetic centers in northern Chile contain two or three plagioclase populations. The first one is characterized by defined edges and no resorption features (**Figure 10e**). The second population of plagioclase show inner zones with sieve texture overgrown by euhedral rims of plagioclase, and plagioclase that is thoroughly sieved (**Figure 10e**). The last population of plagioclase exhibits oscillatory zoning and, in some cases, coarse-sieve texture and smooth edges. The mineral assemblage consists of plagioclase, olivine, orthopyroxene, and clinopyroxene, in order of decreasing abundances, with amphibole and opaque mineral (e.g., magnetite and ilmenite) as minor phases for mafic products, and plagioclase, amphibole, biotite, quartz, K-feldspar, pyroxene, titanite and opaque mineral (e.g., magnetite and ilmenite), in order of decreasing abundances, with apatite and zircon as accessory phases for felsic products. For mafic products, olivines are present in samples showing reabsorption features characterized by different types of skeletal crystal morphologies (**Figure 10f**). Pyroxene is commonly recognized as individual crystal, and as reaction rims on olivine crystals or glomerocrystals. Quartz xenocrysts are also identified and are resorbed and rimmed by a network of mafic microlites (e.g., clinopyroxene) (**Figure 10d**). For felsic products, quartz crystals have rounded edges; amphibole and biotite show euhedral to subhedral habits affected by the intense breakdown (**Figure 10g**). Overall, the groundmass is very finely crystalline, with microlites of plagioclase, ortho- and clinopyroxene, olivine, amphibole, and opaque minerals with interstitial glass (**Figure 10**).

These characteristics correspond to disequilibrium textures, giving evidence of magma mixing, heating of the reservoirs where the crystals are located or assimilation of crustal rocks, fast ascent, cooling, and decompression (e.g. [61]). The mixing processes correspond to mechanical mixing processes or mingling [62], which occur when mafic magma had insufficient interaction time with the felsic magma to generate a chemical mixing [62]. This process occurs at around 0.1–10 km depth [63], developed in different degrees, being evidenced by mafic enclaves (e.g., Tinto dome) and alternating mafic and felsic bands (e.g., El Maní dome) with flow structures [64]. Assimilation and fractional crystallization can be interpreted by the role of amphibole fractionation and plagioclase crystallization, respectively [32]. Whereas, all rims on amphibole and biotite phenocrysts suggest a fast magma ascent as a consequence of decompression [65].

Geochemically, based on the total alkali-silica diagram (after [66]), mafic monogenetic volcanism in northern Chile range mainly from basaltic andesite to dacitic in composition, which corresponds to scoria cones, lava flows, domes, maars, and tuff cones (**Figure 11a**). On the other hand, felsic products range from dacitic to rhyolitic composition, which corresponds to domes (**Figure 11a**). All the samples have calc-alkaline composition (not shown; after [72]), whilst mafic and felsic samples are mainly in the medium-K and high-K fields, respectively (not shown; after [73]). Based on geochemical compositional variations (Sr/Y, Sm/Yb,

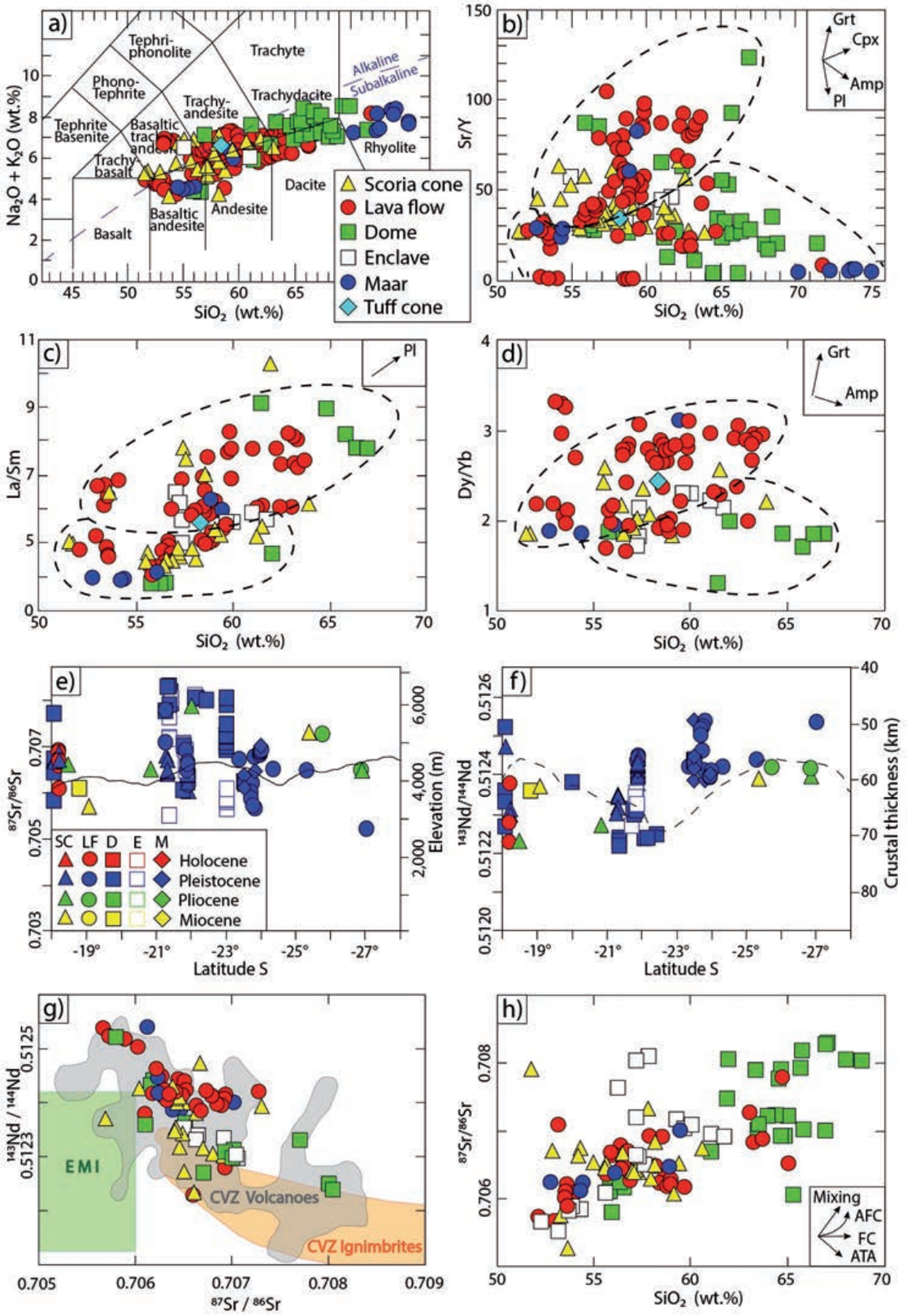

Figure 11.
a) Total alkalis–silica diagram (after [66]). b) SiO_2 vs. Sr./Y diagram. c) SiO_2 vs. La/Sm diagram. d) SiO_2 vs. Dy/Yb diagram. The segmented lines correspond to the two group areas described in the text. e-f) comparison of whole-rock $^{87}Sr/^{86}Sr$ and $^{143}Nd/^{144}Nd$ ratios of monogenetic volcanoes with elevation (continuous line) and crustal thickness (dashed line), respectively. Arc front means elevation and crustal thickness profiles taken from Scott et al. [67]. SC: Scoria cone; LF: Lava flow; D: Dome; E: Enclave; M: Maar. g) $^{87}Sr/^{86}Sr$ vs. $^{143}Nd/^{144}Nd$ diagram; EMI (enriched mantle I) green area from Lucassen et al. [68] and references therein; the gray area from Scott et al. [67] and orange area from Franz et al. [69]. h) $^{87}Sr/^{86}Sr$ vs. SiO_2 diagram. Arrows of differentiation trends (with relative mineral contribution) after Mamani et al. [70] and Delacour et al. [71]. Grt: Garnet; Cpx: Clinopyroxene; amp: Amphibole; Pl: Plagioclase; AFC: Assimilation fractional crystallization; FC: Fractional crystallization; ATA: Assimilation during turbulent magma ascent.

Dy/Yb, and La/Sm ratio contents), monogenetic products can be divided into two types (**Figure 11b-d**). A group with high contents of Sr./Y, Sm/Yb, Dy/Yb, and La/Sm ratio shows deep assimilation under high pressures and thick crust assimilation garnet signature [70]. The second group has low Sr./Y, Sm/Yb, Dy/Yb, and La/Sm ratios, and displays shallow assimilation with amphibole and clinopyroxene fractionation [74].

Eruptive products of monogenetic volcanoes of northern Chile show values between 0.705–0.708 for $^{87}Sr/^{86}Sr$, and 0.5122–0.5126 for $^{143}Nd/^{144}Nd$ (**Figure 11e-g**). These values are higher than expected for magmas derived from the asthenospheric mantle, and relatively restricted compared to isotopic data of stratovolcanoes from the CVZ (**Figure 11e**). Overall, less differentiated products show $^{87}Sr/^{86}Sr$ values lower (< 0.707) than more differentiated products (> 0.707) (**Figure 11e,f**). The $^{87}Sr/^{86}Sr$ vs. SiO_2 diagram shows that assimilation and fractional crystallization (AFC) occur at different degrees and levels during the magmatic ascent from the source to the surface (**Figure 11h**). Fractional crystallization processes characterize these products, with a low degree of contamination and increasing HREE depletion (e.g., Dy, Yb, or Y), which suggest residual garnet of mantle melting enhanced by lithospheric delamination [75]. Nevertheless, a group of samples of mafic lava flows and scoria cones displays a reverse isotopic behavior of decreasing $^{87}Sr/^{86}Sr$ ratio values with the increasing of the SiO_2 (**Figure 11h**). This trend cannot be explicated by mixing processes where is an increase of LILE content compared with HFSE or by AFC processes that expect an enrichment of $^{87}Sr/^{86}Sr$ ratio values during the differentiation [76]. In this context, assimilation during turbulent ascent process has been proposed (ATA; [77, 78]). This ATA process generates a selective fusion and assimilation of felsic crust, enriching of LILE (e.g., Sr or Rb; **Figure 11b**) compared with HFSE (e.g., Y or La; **Figure 11b,c**), and an enrichment of radiogenic strontium (**Figure 11e**, **f**, and **h**) like the more evolved silicic products over a relatively short time [77, 79].

On the other hand, the felsic products can be explained by the presence of a magma reservoir located in the middle-shallow crust (e.g., polybaric crystallization using the amphibole thermobarometer; [80, 81]). Two feeding reservoir systems have been identified for silicic magmas at ~4–8 km depth (~740–840°C) and at ~15–20 km (~940–1000°C) depth, respectively [80, 81]. In addition, melting-assimilation-storage-homogenization (MASH; [76]) zones have been interpreted and identified by petrological and seismic tomographic studies at ~15–40 km depth such as Altiplano-Puna Magma Body (APMB), Lazufre Magma Body (LMB) or Incahuasi Magma Body (IMB) [82–84]. These magmatic reservoirs are associated with a magmatic flare-up and magmatic steady-stage during the formation of the large ignimbrite deposits and growth of stratovolcanoes in northern Chile [85, 86]. This suggests that after these magmatic phases (flare-up and steady stage), the formation of shallow magmatic reservoirs (at 4–8 km depth) could have been formed as remnants of these eruptions. These would have been fed by a magmatic system of super-eruption scale (e.g., APMB, LMB, or IMB) of dacitic magmas and by new magma batches of less-evolved magmas [32, 87], triggering silicic eruptions of large volume with mafic inclusions as enclaves.

Therefore, based on the geochemical and isotopic compositional variations, the monogenetic volcanic products of northern Chile are characterized by two groups of magmas. One of them presents a magma evolution dominated by a high-pressure garnet source at deepest crust levels [71, 88] (**Figure 12**) characterized by different magmatic processes as FC, AFC, and ATA (**Figure 12**). The second group of magmas presents a magma evolution dominated by low-pressure garnet-free source middle-upper crust level to shallow crustal levels. This group of magmas is characterized by crystallizing of amphibole during the magma ascent (e.g. [32, 87]), and by AFC magmatic processes with different mixing degree (**Figure 12**).

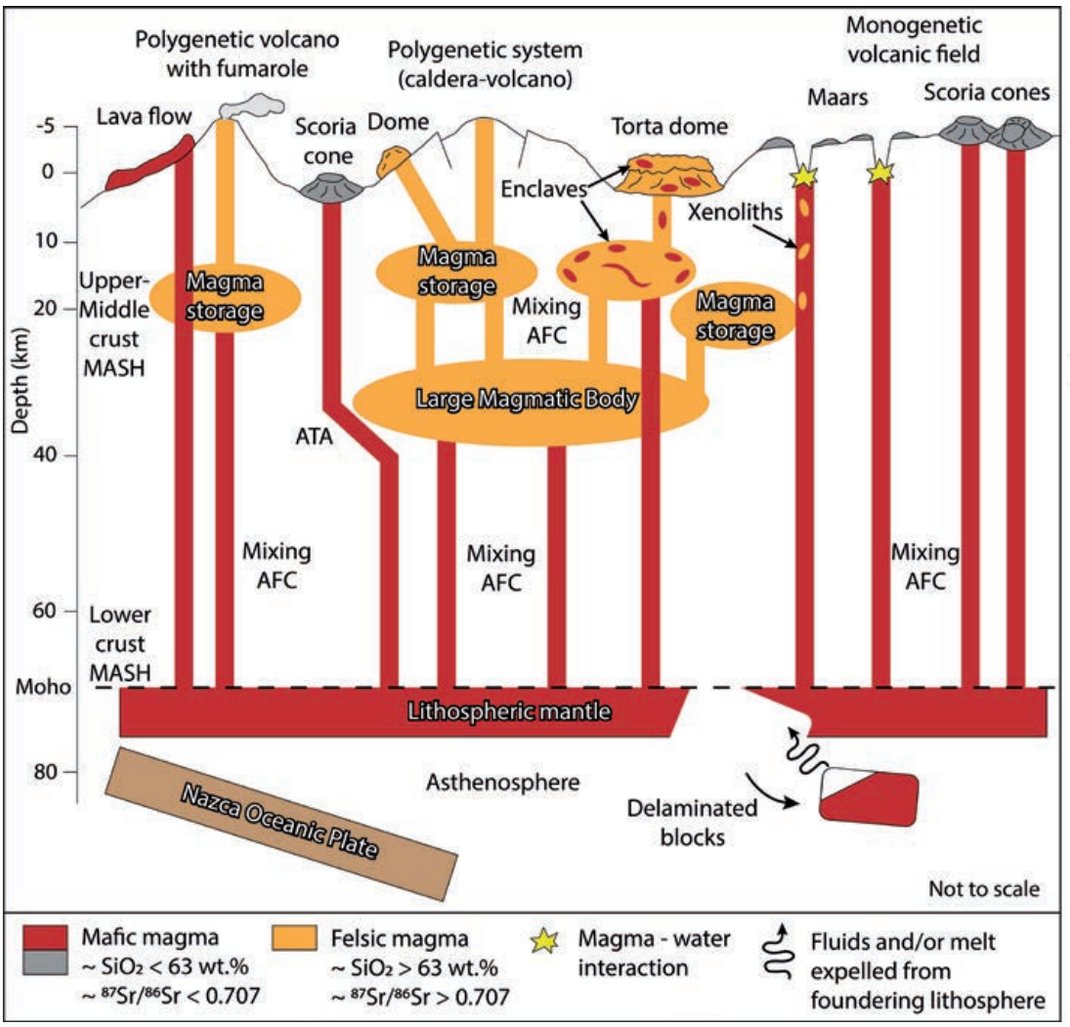

Figure 12.
Conceptual model diagram of the magmatic system for monogenetic volcanoes in northern Chile. This model relates mantle-derived magmas with felsic upper crustal partially molted levels of magma storages such as shallow pre-eruptive reservoirs and large magmatic bodies (e.g., Altiplano-Puna Magma body). Processes during the magma ascent from source to the surface, such as MASH (melting-assimilation-storage-homogenization), mixing, AFC (assimilation fractional crystallization), ATA (assimilation during turbulent magma ascent) or magma-water interaction (phreatomagmatism). Distribution of these zones is constrained by stratigraphic [33–35], petrologic and thermobarometric [29, 79, 87–89], and geophysical [82–84] data. Partial melting and assimilation of lithospheric mantle by delaminated material at the base of the lithosphere model were taken from [75].

6. Concluding remarks

Monogenetic volcanism in northern Chile (18–28° Lat. S) is represented by 907 centers characterized by small (e.g., SC2 scoria cone) and large-volume (e.g., La Torta de Tocorpuri dome) volcanic structures. It exhibits a wide range of composition, from basaltic andesite (e.g., Cerro Overo) to rhyolite (e.g., Corral de Coquena) and a wide spectrum of volcanic landform, lithofacies, and hydromagmatic and magmatic eruptive styles (with the transition from explosive to effusive, and vice versa).

Among these eruptive styles, the most abundant activity corresponds to effusive and Strombolian eruptions. In contrast, the fewer frequency activities are the phreatomagmatic and Surtseyan eruptions (**Figure 3**), which is concordant with an arid climate in northern Chile from the Miocene [41, 90]. This could be related to the degree of glaciation because when everything is too cold and frozen, not a lot of water can infiltrate to become groundwater. At the same time, in warmer periods, meltwater can form lakes or flow toward basins from the peaks.

Although the numbers of monogenetic volcanoes represented in this contribution are limited by the exposure, and more features could be hidden by Neogene sedimentary and volcanic cover. Monogenetic volcanoes were mainly emplaced during Pleistocene and Miocene, generating scoria cones, domes, lava flows, maars, and tuff cones, in order to decrease. The relative abundance of volcanic features is, in part, limited by the amount of time for eruptions, where the spike in the Pleistocene is prominent, for being a short time period (~2 Ma). While the preservation of Miocene features is also notable in that they are still accessible favored by the arid climate in northern Chile from the Miocene.

Spatially, monogenetic volcanoes are mainly associated with NW-striking lineaments or with the intersections of NW-striking lineaments, NNW-to-NNE-striking faults, and WNW-striking lineaments, in decreasing order. Although the main tectonic setting in northern Chile corresponds to the compressional environment, tectonic phases of Quaternary crustal relaxation (neutral to extensional stresses) could have favored the rising of magmas in small batches up from the source (deep or shallow) to the surface.

A general eruptive model for monogenetic volcanoes in northern Chile is proposed in this work, where the external (e.g., magma reservoirs or groundwater availability) and internal (e.g., magma ascent rate or interaction *en-route* to the surface) conditions determine the changes in eruptive style, lithofacies, and magmatic processes involved in the formation of monogenetic volcanoes. Especially during explosive volcanic eruptions, which involve interaction with water, the resulting volcanic lithofacies and architecture will be diverse, reflecting the potential hazards that future eruptions could generate. The understanding of the tectonic and hydrologic setting of the region using traditional geophysics and volcanology surveys should play an essential role in volcanic monitoring, particularly in localities of the Altiplano (e.g., Ollagüe and Talabre village) located nearby active stratovolcanoes presenting permanent fumarolic activity (e.g., Guallatiri, Ollagüe or Lascar stratovolcanoes). This is especially important if such monogenetic volcanoes are surrounded by water-saturated high altitude sedimentary basins, such as salt flats (e.g., Salar de Carcote, Lejía, or Chungara lakes), where even a small-volume of any type of magma ascent could erupt in complex volcanic eruptions in northern Chile.

7. Supplementary data

Methods and databases (Table A.1. Monogenetic volcanoes location database; Table A.2. Geochronological database; Table A.3. Geochemical database; Figure A.1. Structural styles of monogenetic volcanoes in northern Chile; Figure A.2. Tectonic structures and lineaments database). https://drive.google.com/drive/u/1/folders/1dwmvUiYTMF-XOoDXTwPhRYyHy88wNehJ.

Acknowledgements

The authors wish to thank the Collaborative Research Center 1211–Earth Evolution at the Dry Limit and Dr. Eduardo Campos for providing the vehicle used during fieldwork. The authors would also like to thank all members of the Núcleo de Investigación en Riesgo Volcánico - Ckelar Volcanes team for fruitful discussions and support during fieldwork. The authors highly appreciate the time and effort of Dr. Alison Graettinger for her comments to improve this contribution.

Funding

This research is part of G.U. Ph.D. thesis, which is funded by CONICYT-PCHA Doctorado Nacional 2016–21161286 fellowship and supported by the Universidad Católica del Norte. This study is emerged and funded by CONICYT-PAI MEC 2017–80170048 (titled "Fortalecimiento del área de volcanismo en el Departamento de Ciencias Geológicas"), and the Antofagasta Regional Government, FIC-R project, code BIP Nº30488832-0 (titled "Mitigación del riesgo asociado a procesos volcánicos en la Región de Antofagasta"); based on the Memorandum of Understanding of Research Cooperation between Universidad Católica del Norte and Massey University.

Conflict of interest

There are no conflicts of interest.

Author details

Gabriel Ureta[1,2,3*], Károly Németh[4], Felipe Aguilera[1,3,5], Matias Vilches[1,5], Mauricio Aguilera[1,5], Ivana Torres[1], José Pablo Sepúlveda[1,6], Alexander Scheinost[1,2] and Rodrigo González[1,5]

1 Núcleo de Investigación en Riesgo Volcánico - Ckelar Volcanes, Universidad Católica del Norte, Antofagasta, Chile

2 Universidad Católica del Norte, Programa de Doctorado en Ciencias Mención Geología, Antofagasta, Chile

3 Centro Nacional de Investigación para la Gestión Integrada del Riesgo de Desastres (CIGIDEN), Santiago, Chile

4 Volcanic Risk Solutions, School of Agriculture and Environment, Massey University, Palmerston North, New Zealand

5 Universidad Católica del Norte, Departamento de Ciencias Geológicas, Antofagasta, Chile

6 Dipartimento di Scienze della Terra, Università degli Studi di Firenze, Florence, Italy

*Address all correspondence to: gabriel.ureta@ucn.cl

References

[1] Valentine GA, Gregg TKP. Continental basaltic volcanoes — Processes and problems. Journal of Volcanology and Geothermal Research. 2008; 177: 857-873. 10.1016/j.jvolgeores.2008.01.050

[2] Le Corvec N, Spörli KB, Rowland J, Lindsay J. Spatial distribution and alignments of volcanic centers: Clues to the formation of monogenetic volcanic fields. Earth-Science Reviews. 2013; 124: 96-114. 10.1016/j.earscirev.2013.05.005

[3] Haag MB, Baez WA, Sommer CA, Arnosio JM, Filipovich RE. Geomorphology and spatial distribution of monogenetic volcanoes in the southern Puna Plateau (NW Argentina). Geomorphology. 2019; 342: 196-209. https://doi.org/10.1016/j.geomorph.2019.06.008

[4] de Silva SL. Altiplano-Puna volcanic complex of the central Andes. Geology. 1989; 17: 1102-1106. 10.1130/0091-7613(1989)017<1102:Apvcot>2.3.Co;2

[5] Smith IEM, Németh K. Source to surface model of monogenetic volcanism: a critical review. In: Monogenetic Volcanism (eds Németh K, Carrasco-Núñez G, Aranda-Gómez JJ, Smith IEM). Geological Society (2017). 1-28. doi.org/10.1144/sp446.14

[6] Kereszturi G, Németh K. Monogenetic Basaltic Volcanoes: Genetic Classification, Growth, Geomorphology and Degradation. In: Updates in Volcanology - New Advances in Understanding Volcanic Systems (ed Németh K). Intech Open (2012). 3-88 10.5772/51387

[7] Németh K, Kereszturi G. Monogenetic volcanism: personal views and discussion. International Journal of Earth Sciences. 2015; 104: 2131-2146. doi.org/10.1007/s00531-015-1243-6

[8] Hopkins JL, Smid ER, Eccles JD, Hayes JL, Hayward BW, McGee LE, van Wijk K, Wilson TM, Cronin SJ, Leonard GS, Lindsay JM, Németh K, Smith IEM. Auckland Volcanic Field magmatism, volcanism, and hazard: a review. New Zealand Journal of Geology and Geophysics. 2020: 1-22. 10.1080/00288306.2020.1736102

[9] Thorpe RS, Francis PW. Variations in andean andesite compositions and their petrogenetic significance. Tectonophysics. 1979; 57: 53-70. https://doi.org/10.1016/0040-1951(79)90101-X

[10] de Silva SL, Francis PW. Volcanoes of the central Andes. Springer-Verlag (1991).

[11] Global Volcanism Program. Volcanoes of the World, v. 4.8.5. In: Smithsonian Institution (ed Venzke Ee) (2013).

[12] Trumbull RB, Riller U, Oncken O, Scheuber E, Munier K, Hongn F. The Time-Space Distribution of Cenozoic Volcanism in the South-Central Andes: a New Data Compilation and Some Tectonic Implications. In: The Andes: Active Subduction Orogeny (eds Oncken O, *et al.*). Springer Berlin Heidelberg (2006). 29-43. 10.1007/978-3-540-48684-8_2

[13] Hora JM, Singer BS, Worner G. Volcano evolution and eruptive flux on the thick crust of the Andean Central Volcanic Zone: 40Ar/39Ar constraints from Volcan Parinacota, Chile. Geological Society of America Bulletin. 2007; 119: 343-362. 10.1130/b25954.1

[14] Inostroza M, Aguilera F, Menzies A, Layana S, González C, Ureta G, Sepúlveda J, Scheller S, Böehm S, Barraza M, Tagle R, Patzschke M. Deposition of metals and metalloids in the fumarolic fields of Guallatiri and Lastarria volcanoes, northern Chile. Journal of Volcanology and Geothermal Research. 2020; 393: 106803. https://doi.org/10.1016/j.jvolgeores.2020.106803

[15] Klemetti EW, Grunder AL. Volcanic evolution of Volcán Aucanquilcha: a long-lived dacite volcano in the Central Andes of northern Chile. Bulletin of Volcanology. 2008; 70: 633-650. 10.1007/s00445-007-0158-x

[16] Vezzoli L, Tibaldi A, Renzulli A, Menna M, Flude S. Faulting-assisted lateral collapses and influence on shallow magma feeding system at Ollagüe volcano (Central Volcanic Zone, Chile-Bolivia Andes). Journal of Volcanology and Geothermal Research. 2008; 171: 137-159. 10.1016/j.jvolgeores.2007.11.015

[17] Calder ES, Sparks RSJ, Gardeweg MC. Erosion, transport and segregation of pumice and lithic clasts in pyroclastic flows inferred from ignimbrite at Lascar Volcano, Chile. Journal of Volcanology and Geothermal Research. 2000; 104: 201-235. https://doi.org/10.1016/S0377-0273(00)00207-9

[18] Francis PW, Gardeweg M, Ramirez CF, Rothery DA. Catastrophic debris avalanche deposit of Socompa volcano, northern Chile. Geology. 1985; 13: 600-603. 10.1130/0091-7613(1985)13<600:cdados>2.0.co;2

[19] Aguilera F, Layana S, Rodríguez-Díaz A, González C, Cortés J, Inostroza M. Hydrothermal alteration, fumarolic deposits and fluids from Lastarria Volcanic Complex: A multidisciplinary study. Andean Geology. 2016; 43: 166-196.

[20] Baker PE, Gonzalez-Ferran O, Rex DC. Geology and geochemistry of the Ojos del Salado volcanic region, Chile. Journal of the Geological Society. 1987; 144: 85-96. 10.1144/gsjgs.144.1.0085

[21] de Silva SL, Self S, Francis PW, Drake RE, Carlos RR. Effusive silicic volcanism in the Central Andes: The Chao dacite and other young lavas of the Altiplano-Puna Volcanic Complex. Journal of Geophysical Research: Solid Earth. 1994; 99: 17805-17825. 10.1029/94jb00652

[22] González G, Cembrano J, Aron F, Veloso EE, Shyu JBH. Coeval compressional deformation and volcanism in the central Andes, case studies from northern Chile (23°S–24°S). Tectonics. 2009; 28: TC6003. https://doi.org/10.1029/2009TC002538

[23] Cornejo PN, J.A. Azufrera Juan de la Vega: un maar de origen freatomagmático, Andes del norte de Chile (25°52'S). . In: ^V Congreso Geológico de Chile; Santiago, Chile); 209-227

[24] Self S, de Silva SL, Cortés JA. Enigmatic clastogenic rhyolitic volcanism: The Corral de Coquena spatter ring, North Chile. Journal of Volcanology and Geothermal Research. 2008; 177: 812-821. 10.1016/j.jvolgeores.2008.01.047

[25] Mattioli M, Renzulli A, Menna M, Holm PM. Rapid ascent and contamination of magmas through the thick crust of the CVZ (Andes, Ollagüe region): Evidence from a nearly aphyric high-K andesite with skeletal olivines. Journal of Volcanology and Geothermal Research. 2006; 158: 87-105. 10.1016/j.jvolgeores.2006.04.019

[26] Watts RB, Clavero Ribes J, Sparks RSJ. The origin and emplacement of Domo Tinto, Guallatiri volcano, Northern Chile. Andean Geology. 2014; 41. 10.5027/andgeoV41n3-a04

[27] Godoy B, Taussi M, González-Maurel O, Renzulli A, Hernández-Prat L, le Roux P, Morata D, Menzies A. Linking the mafic volcanism with the magmatic stages during the last 1 Ma in the main volcanic arc of the Altiplano-Puna Volcanic Complex (Central Andes). Journal of South American Earth Sciences. 2019; 95: 102295. https://doi.org/10.1016/j.jsames.2019.102295

[28] Davidson JP, Harmon RS, Wörner G. The source of central Andean magmas; Some considerations. In: Andean magmatism and its tectonic setting). Geological Society of America (1991). 233. 10.1130/SPE265-p233

[29] Burns DH, de Silva SL, Tepley F, Schmitt AK, Loewen MW. Recording the transition from flare-up to steady-state arc magmatism at the Purico–Chascon volcanic complex, northern Chile. Earth and Planetary Science Letters. 2015; 422: 75-86. https://doi.org/10.1016/j.epsl.2015.04.002

[30] van Alderwerelt BMEdR. Diverse monogenetic volcanism across the main arc of the central Andes, northern Chile. [PhD Thesis]. Iowa: University of Iowa; 2017.

[31] González-Maurel O, Godoy B, le Roux P, Rodríguez I, Marín C, sMenzies A, Bertin D, Morata D, Vargas M. Magmatic differentiation at La Poruña scoria cone, Central Andes, northern Chile: Evidence for assimilation during turbulent ascent processes, and genetic links with mafic eruptions at adjacent San Pedro volcano. Lithos. 2019; 338-339: 128-140. https://doi.org/10.1016/j.lithos.2019.03.033

[32] Taussi M, Godoy B, Piscaglia F, Morata D, Agostini S, Le Roux P, Gonzalez-Maurel O, Gallmeyer G, Menzies A, Renzulli A. The upper crustal magma plumbing system of the Pleistocene Apacheta-Aguilucho Volcanic Complex area (Altiplano-Puna, northern Chile) as inferred from the erupted lavas and their enclaves. Journal of Volcanology and Geothermal Research. 2019; 373: 179-198. https://doi.org/10.1016/j.jvolgeores.2019.01.021

[33] Torres I, Németh K, Ureta G, Aguilera F. Characterization, origin, and evolution of one of the most eroded mafic monogenetic fields within the central Andes: The case of El País lava flow field, northern Chile. Journal of South American Earth Sciences. 2020:102942. https://doi.org/10.1016/j.jsames.2020.102942

[34] Ureta G, Németh K, Aguilera F, Kósik S, González R, Menzies A, González C, James D. Evolution of a magmatic explosive/effusive to phreatomagmatic volcanic system: birth of a monogenetic volcanic field, Tilocálar volcanoes, northern Chile. Journal of Volcanology and Geothermal Research. Unpublished.

[35] Ureta G, Aguilera F, Németh K, Inostroza M, González C, Zimmer M, Menzies A. Transition from small-volume ephemeral lava emission to explosive hydrovolcanism: The case of Cerro Tujle maar, northern Chile. Journal of South American Earth Sciences. 2020; 104: 102885. https://doi.org/10.1016/j.jsames.2020.102885

[36] Wörner G, Schildgen TF, Reich M. The Central Andes: Elements of an Extreme Land. Elements. 2018; 14: 225-230. 10.2138/gselements.14.4.225

[37] Yuan X, Sobolev SV, Kind R. Moho topography in the central Andes and its geodynamic implications. Earth and Planetary Science Letters. 2002; 199: 389-402. https://doi.org/10.1016/S0012-821X(02)00589-7

[38] Beck SL, Zandt G, Myers SC, Wallace TC, Silver PG, Drake L. Crustal-thickness variations in the central Andes. Geology. 1996; 24: 407-410. 10.1130/0091-7613(1996)024<0407:ctvitc>2.3.co;2

[39] Schmitz M, Heinsohn WD, Schilling FR. Seismic, gravity and petrological evidence for partial melt beneath the thickened Central Andean crust (21-23°S). Tectonophysics. 1997; 270: 313-326. https://doi.org/10.1016/S0040-1951(96)00217-X

[40] Kay SM, Coira B, Viramonte J. Young mafic back arc volcanic rocks as

indicators of continental lithospheric delamination beneath the Argentine Puna Plateau, central Andes. Journal of Geophysical Research: Solid Earth. 1994; 99: 24323-24339. doi:10.1029/94JB00896

[41] Lamb S, Davis P. Cenozoic climate change as a possible cause for the rise of the Andes. Nature. 2003; 425: 792-797. 10.1038/nature02049

[42] Wörner G, Hammerschmidt K, Henjes-Kunst F, Lezaun J, Wilke H. Geochronology (40Ar/39Ar, K-Ar and He-exposure ages) of Cenozoic magmatic rocks from Northern Chile (18-22°S): implications for magmatism and tectonic evolution of the central Andes. Revista geológica de Chile. 2000; 27: 205-240.

[43] Stern CR. Active Andean volcanism: its geologic and tectonic setting. Revista geológica de Chile. 2004; 31: 161-206.

[44] González-Ferrán O. Volcanes de Chile. Instituto Geográfico Militar (1995).

[45] De la Cruz-Reyna S, Yokoyama I. A geophysical characterization of monogenetic volcanism. Geofísica internacional. 2011; 50: 465-484.

[46] Bishop MA. Point pattern analysis of eruption points for the Mount Gambier volcanic sub-province: a quantitative geographical approach to the understanding of volcano distribution. Area. 2007; 39: 230-241. 10.1111/j.1475-4762.2007.00729.x

[47] Pardo-Casas F, Molnar P. Relative motion of the Nazca (Farallon) and South American Plates since Late Cretaceous time. Tectonics. 1987; 6: 233-248. 10.1029/TC006i003p00233

[48] Tibaldi A, Bonali FL. Contemporary recent extension and compression in the central Andes. Journal of Structural Geology. 2018; 107: 73-92. 10.1016/j.jsg.2017.12.004

[49] Tibaldi A, Bonali FL, Corazzato C. Structural control on volcanoes and magma paths from local- to orogen-scale: The central Andes case. Tectonophysics. 2017; 699: 16-41. 10.1016/j.tecto.2017.01.005

[50] Tibaldi A, Corazzato C, Rovida A. Miocene–Quaternary structural evolution of the Uyuni–Atacama region, Andes of Chile and Bolivia. Tectonophysics. 2009; 471: 114-135. 10.1016/j.tecto.2008.09.011

[51] González-Ferrán O, Baker PE, Rex DC. Tectonic-volcanic discontinuity at latitude 27° south Andean Range, associated with Nazca Plate Subduction. Tectonophysics. 1985; 112: 423-441. doi.org/10.1016/0040-1951(85)90189-1

[52] Báez W, Carrasco Nuñez G, Giordano G, Viramonte JG, Chiodi A. Polycyclic scoria cones of the Antofagasta de la Sierra basin, Southern Puna plateau, Argentina. In: Monogenetic Volcanism (eds Németh K, Carrasco-Núñez G, Aranda-Gómez JJ, Smith IEM). Geological Society (2017). 311-336. 10.1144/sp446.3

[53] Bishop MA. A generic classification for the morphological and spatial complexity of volcanic (and other) landforms. Geomorphology. 2009; 111: 104-109. https://doi.org/10.1016/j.geomorph.2008.10.020

[54] Walker GPL. Compound and simple lava flows and flood basalts. Bulletin Volcanologique. 1971; 35: 579-590. 10.1007/bf02596829

[55] Burgisser A, Degruyter W. Magma Ascent and Degassing at Shallow Levels. In: The Encyclopedia of Volcanoes (Second Edition) (eds Sigurdsson H, Houghton B, McNutt SR, Rymer H, Stix J). Academic Press (2015). 225-236. 10.1016/b978-0-12-385938-9.00011-0

[56] Cassidy M, Manga M, Cashman K, Bachmann O. Controls on explosive-effusive volcanic eruption styles.

Nature Communications. 2018; 9: 2839. 10.1038/s41467-018-05293-3

[57] Németh K, Kósik S. Review of Explosive Hydrovolcanism. Geosciences. 2020; 10: 44.

[58] de Silva S, Lindsay JM. Primary Volcanic Landforms. In: The Encyclopedia of Volcanoes (Second Edition) (eds Sigurdsson H, Houghton B, McNutt SR, Rymer H, Stix J). Academic Press (2015). 273-297. 10.1016/b978-0-12-385938-9.00015-8

[59] Maro G, Caffe PJ. Neogene monogenetic volcanism from the Northern Puna region: products and eruptive styles. In: Monogenetic Volcanism (eds Németh K, Carrasco-Núñez G, Aranda-Gómez JJ, Smith IEM). Geological Society (2016). 337-359. 10.1144/sp446.6

[60] Maro G, Caffe PJ, Báez W. Volcanismo monogenético máfico cenozoico de la Puna. In: ^Ciencias de la Tierra y Recursos Naturales del NOA. Relatorio del XX Congreso Geológico Argentino San Miguel de Tucumán, Argentina); 548-577

[61] Sosa-Ceballos G, Macías JL, García-Tenorio F, Layer P, Schaaf P, Solís-Pichardo G, Arce JL. El Ventorrillo, a paleostructure of Popocatépetl volcano: insights from geochronology and geochemistry. Bulletin of Volcanology. 2015; 77: 91. 10.1007/s00445-015-0975-2

[62] Barbarin B, Didier J. Genesis and evolution of mafic microgranular enclaves through various types of interaction between coexisting felsic and mafic magmas. Earth and Environmental Science Transactions of the Royal Society of Edinburgh. 1992; 83: 145-153. 10.1017/S0263593300007835

[63] De Campos CP, Perugini D, Ertel-Ingrisch W, Dingwell DB, Poli G. Enhancement of magma mixing efficiency by chaotic dynamics: an experimental study. Contributions to Mineralogy and Petrology. 2011; 161: 863-881. 10.1007/s00410-010-0569-0

[64] Perugini D, Poli G. The mixing of magmas in plutonic and volcanic environments: Analogies and differences. Lithos. 2012; 153: 261-277. https://doi.org/10.1016/j.lithos.2012.02.002

[65] Rutherford MJ. Magma Ascent Rates. Reviews in Mineralogy and Geochemistry. 2008; 69: 241-271. 10.2138/rmg.2008.69.7

[66] Le Maitre RW, Bateman P, Dudek A, Keller J, Lameyre J, Le Bas MJ, Sabine PA, Schmid R, Sorensen H, Strekeisen A, Woolley AR, Zanettin B. A classification of igneous rocks and glossary of terms: recommendations of the International Union of Geological Sciences, Subcommission on the Systematics of Igneous Rocks. International Union of Geological Sciences (1989).

[67] Scott EM, Allen MB, Macpherson CG, McCaffrey KJW, Davidson JP, Saville C, Ducea MN. Andean surface uplift constrained by radiogenic isotopes of arc lavas. Nature Communications. 2018; 9: 969. 10.1038/s41467-018-03173-4

[68] Lucassen F, Kramer W, Bartsch V, Wilke H-G, Franz G, Romer RL, Dulski P. Nd, Pb, and Sr isotope composition of juvenile magmatism in the Mesozoic large magmatic province of northern Chile (18-27°S): indications for a uniform subarc mantle. Contributions to Mineralogy and Petrology. 2006; 152: 571. 10.1007/s00410-006-0119-y

[69] Franz G, Lucassen F, Kramer W, Trumbull RB, Romer RL, Wilke H-G, Viramonte JG, Becchio R, Siebel W. Crustal Evolution at the Central Andean Continental Margin: a Geochemical Record of Crustal Growth, Recycling

and Destruction. In: The Andes: Active Subduction Orogeny (eds Oncken O, *et al.*). Springer Berlin Heidelberg (2006). 45-64. 10.1007/978-3-540-48684-8_3

[70] Mamani M, Worner G, Sempere T. Geochemical variations in igneous rocks of the Central Andean orocline (13 S to 18 S): Tracing crustal thickening and magma generation through time and space. Geological Society of America Bulletin. 2010; 122: 162-182. 10.1130/b26538.1

[71] Delacour A, Gerbe M-C, Thouret J-C, Wörner G, Paquereau-Lebti P. Magma evolution of Quaternary minor volcanic centres in southern Peru, Central Andes. Bulletin of Volcanology. 2007; 69: 581-608. 10.1007/s00445-006-0096-z

[72] Irvine TN, Baragar WRA. A Guide to the Chemical Classification of the Common Volcanic Rocks. Canadian Journal of Earth Sciences. 1971; 8: 523-548. https://doi.org/10.1139/e71-055

[73] Peccerillo A, Taylor SR. Geochemistry of eocene calc-alkaline volcanic rocks from the Kastamonu area, Northern Turkey. Contributions to Mineralogy and Petrology. 1976; 58: 63-81. https://doi.org/10.1007/bf00384745

[74] Wörner G, Mamani M, Blum-Oeste M. Magmatism in the Central Andes. Elements. 2018; 14: 237-244. 10.2138/gselements.14.4.237

[75] Murray KE, Ducea MN, Schoenbohm L. Foundering-driven lithospheric melting: The source of central Andean mafic lavas on the Puna Plateau (22 S–27 S). Geodynamics of a Cordilleran Orogenic System: The Central Andes of Argentina and Northern Chile: Geological Society of America Memoir. 2015; 212: 139-166.

[76] Hildreth W, Moorbath S. Crustal contributions to arc magmatism in the Andes of Central Chile. Contributions to Mineralogy and Petrology. 1988; 98: 455-489. 10.1007/bf00372365

[77] Huppert HE, Stephen R, Sparks J. Cooling and contamination of mafic and ultramafic magmas during ascent through continental crust. Earth and Planetary Science Letters. 1985; 74: 371-386. https://doi.org/10.1016/S0012-821X(85)80009-1

[78] Kerr AC, Kempton PD, Thompson RN. Crustal assimilation during turbulent magma ascent (ATA); new isotopic evidence from the Mull Tertiary lava succession, N. W. Scotland. Contributions to Mineralogy and Petrology. 1995; 119: 142-154. 10.1007/BF00307277

[79] Maro G, Caffe PJ, Romer RL, Trumbull RB. Neogene Mafic Magmatism in the Northern Puna Plateau, Argentina: Generation and Evolution of a Back-arc Volcanic Suite. Journal of Petrology. 2017; 58: 1591-1617. 10.1093/petrology/egx066

[80] Gorini A, Ridolfi F, Piscaglia F, Taussi M, Renzulli A. Application and reliability of calcic amphibole thermobarometry as inferred from calc-alkaline products of active geothermal areas in the Andes. Journal of Volcanology and Geothermal Research. 2018; 358: 58-76. https://doi.org/10.1016/j.jvolgeores.2018.03.018

[81] Ridolfi F, Renzulli A, Puerini M. Stability and chemical equilibrium of amphibole in calc-alkaline magmas: an overview, new thermobarometric formulations and application to subduction-related volcanoes. Contributions to Mineralogy and Petrology. 2010; 160: 45-66. 10.1007/s00410-009-0465-7

[82] Zandt G, Leidig M, Chmielowski J, Baumont D, Yuan X. Seismic Detection and Characterization of the

Altiplano-Puna Magma Body, Central Andes. pure and applied geophysics. 2003; 160: 789-807. 10.1007/pl00012557

[83] Kay SM, Mpodozis C, Gardeweg M. Magma sources and tectonic setting of Central Andean andesites (25.5-28°S) related to crustal thickening, forearc subduction erosion and delamination. In: Orogenic Andesites and Crustal Growth (eds Gómez-Tuena A, Straub SM, Zellmer GF). Geological Society (2013). 303-334. 10.1144/sp385.11

[84] Ward KM, Delph JR, Zandt G, Beck SL, Ducea MN. Magmatic evolution of a Cordilleran flare-up and its role in the creation of silicic crust. Scientific Reports. 2017; 7: 9047. 10.1038/s41598-017-09015-5

[85] de Silva SL, Riggs NR, Barth AP. Quickening the Pulse: Fractal Tempos in Continental Arc Magmatism. Elements. 2015; 11: 113-118. 10.2113/gselements.11.2.113

[86] Perkins JP, Ward KM, de Silva SL, Zandt G, Beck SL, Finnegan NJ. Surface uplift in the Central Andes driven by growth of the Altiplano Puna Magma Body. Nat Commun. 2016; 7: 13185. 10.1038/ncomms13185

[87] Godoy B, McGee L, González-Maurel O, Rodríguez I, le Roux P, Morata D, Menzies A. Upper crustal differentiation processes and their role in 238U-230Th disequilibria at the San Pedro-Linzor volcanic chain (Central Andes). Journal of South American Earth Sciences. 2020; 102: 102672. https://doi.org/10.1016/j.jsames.2020.102672

[88] González-Maurel O, le Roux P, Godoy B, Troll VR, Deegan FM, Menzies A. The great escape: Petrogenesis of low-silica volcanism of Pliocene to Quaternary age associated with the Altiplano-Puna Volcanic Complex of northern Chile (21°10′-22°50′S). Lithos. 2019; 346-347: 105162. https://doi.org/10.1016/j.lithos.2019.105162

[89] de Silva SL, Kay SM. Turning up the Heat: High-Flux Magmatism in the Central Andes. Elements. 2018; 14: 245-250. https://doi.org/10.2138/gselements.14.4.245

[90] Vandervoort DS, Jordan TE, Zeitler PK, Alonso RN. Chronology of internal drainage development and uplift, southern Puna plateau, Argentine central Andes. Geology. 1995; 23: 145-148. 10.1130/0091-7613(1995)023<0145:coidda>2.3.co;2